eNeuro

Research Article: New Research | Sensory and Motor Systems

Lack of CaBP1/caldendrin or CaBP2 leads to altered ganglion cell responses

CaBP1 and CaBP2 are important for retinal function

Raunak Sinha[1], Amy Lee[2], Fred Rieke[1] and Francoise Haeseleer[3]

[1]*Dept. of Physiology and Biophysics, Howard Hughes Medical Institute, University of Washington, Seattle, WA 98195*

[2]*Depts. of Molecular Physiology & Biophysics, Otolaryngology Head-Neck Surgery, and Neurology, University of Iowa, Iowa City, IA 52242*

[3]*Dept. of Physiology and Biophysics, University of Washington, Seattle, WA 98195*

DOI: 10.1523/ENEURO.0099-16.2016

Received: 27 April 2016

Revised: 24 September 2016

Accepted: 8 October 2016

Published: 20 October 2016

Author Contributions: RS, FR and FH designed and performed research and analyzed the data. AL contributes unpublished reagents. All authors contributed to writing and approval of the final manuscript.

Funding: Human Frontier Science Program (HFSP): 501100000854; long term fellowship. NIH: R01 EY020850. University of Washington: Royalty Research Fund. University of Washington: Bridge Funding. NIH: EY11850. Howard Hughes Medical Institute; NIH: NS084190. NIH: DC009433. Carver Research Program of Excellence;

Conflict of Interest: The authors report no conflict of interest.

Correspondence should be addressed to Françoise Haeseleer, University of Washington, Department of Hematology, 1705 NE Pacific Street - Box 357710, Seattle, WA 98195, E-mail: fanfan@u.washington.edu

Cite as: eNeuro 2016; 10.1523/ENEURO.0099-16.2016

Manuscript ID: eN-NWR-0099-16

Title page

1. Manuscript Title

Lack of CaBP1/caldendrin or CaBP2 leads to altered ganglion cell responses.

2. Abbreviated Title

CaBP1 and CaBP2 are important for retinal function

3. List all Author Names and Affiliations in order as they would appear in the published article

Raunak Sinha[1], Amy Lee[2], Fred Rieke[1], Francoise Haeseleer[3*]

[1]Dept. of Physiology and Biophysics, Howard Hughes Medical Institute, University of Washington, Seattle, WA 98195

[2]Depts. of Molecular Physiology & Biophysics, Otolaryngology Head-Neck Surgery, and Neurology, University of Iowa, Iowa City, IA 52242

[3]Dept. of Physiology and Biophysics, University of Washington, Seattle, WA 98195

[*] To whom correspondence should be addressed:

Françoise Haeseleer, University of Washington, Department of Hematology, 1705 NE Pacific Street - Box 357710, Seattle, WA 98195, USA, Tel.: (206) 543-2952, Fax: (206) 616-8298, Email: fanfan@u.washington.edu

4. Author Contributions:

RS, FR and FH designed and performed research and analyzed the data. AL contributes unpublished reagents. All authors contributed to writing and approval of the final manuscript.

5. Correspondence should be addressed to (include email address)

Françoise Haeseleer, University of Washington, Department of Hematology, 1705 NE Pacific Street - Box 357710, Seattle, WA 98195, USA, Tel.: (206) 543-2952, Fax: (206) 616-8298, Email: fanfan@u.washington.edu

6. Number of Figures: 11

7. Number of Tables: 2

8. Number of Multimedia: 0

9. Number of words for Abstract: 184

10. Number of words for Significance Statement: 103

11. Number of words for Introduction: 667

12. Number of words for Discussion: 1429

13. Acknowledgements:

We thank Edward Parker at the University of Washington for his great expertise and help with transmission electron microscopy. We thank Jacqueline Mudd at the Embryonic Stem Cell Core-Siteman Cancer Center and Renate Lewis at the Hope Center Transgenic Vectors Core at the Washington University in St. Louis and Robert Hunter at the University of Washington Transgenic Resource Program for their expert work in generating the CaBP2 KO mice. We thank Rachel Wong (University of Washington, Seattle, WA) for the gustducin-GFP mouse retinas, the Zebrafish International Resource Center supported by #RR12546 (NIH-NCRR) for the anti-synaptotagmin 2 antibody, Dr. Arlene Hirano (UCLA, Los Angeles, CA) for the anti-NK3R antibody and Dr. Roger Tsien (HHMI, University of California San Diego, CA) for td-tomato.

14. Conflict of Interest

The authors report no conflict of interest.

15. Funding sources

The research was supported by a University of Washington Royalty Research Fund, University of Washington bridge funding and NIH grant R01 EY020850 to FH, the Howard Hughes Medical Institute and NIH grant EY11850 to FR, NIH grants NS084190 and DC009433 and a Carver Research Program of Excellence to AL and a long-term fellowship by Human Frontier Science Program to RS.

Lack of CaBP1/caldendrin or CaBP2 leads to altered ganglion cell responses.

Abstract

Calcium-binding proteins (CaBPs) form a subfamily of calmodulin-like proteins that were cloned from the retina. CaBP4 and CaBP5 have been shown to be important for normal visual function. Although CaBP1/caldendrin and CaBP2 have been shown to modulate various targets in vitro, it is not known if they contribute to the transmission of light responses through the retina. Therefore, we generated mice that lack CaBP2 or CaBP1/caldendrin (*Cabp2*$^{-/-}$ and *Cabp1*$^{-/-}$) to test if these CaBPs are essential for normal retinal function. By immunohistochemistry, the overall morphology of *Cabp1*$^{-/-}$ and *Cabp2*$^{-/-}$ retinas and the number of synaptic ribbons appear normal; transmission electron microscopy shows normal tethered ribbon synapses and synaptic vesicles as in wild-type retina. However, whole-cell patch clamp recordings showed that light responses of retinal ganglion cells of *Cabp2*$^{-/-}$ and *Cabp1*$^{-/-}$ mice differ in amplitude and kinetics from those of wild-type mice. We conclude that CaBP1/caldendrin and CaBP2 are not required for normal gross retinal and synapse morphology but are necessary for the proper transmission of light responses through the retina; like other CaBPs, CaBP1/caldendrin and CaBP2 likely act by modulating presynaptic Ca^{2+}-dependent signaling mechanisms.

Significance statement

Electrical signals generated by the photoreceptors in response to incident light are processed by diverse retinal neurons before being sent to the brain. Ca^{2+} signaling controls both cellular and synaptic mechanisms that shape signals as they are transmitted through the retina. Ca^{2+}-binding proteins, including the calmodulin-like CaBPs, exert Ca^{2+}-dependent effects on specific target proteins—e.g. ion channels. To determine whether CaBP1/caldendrin and CaBP2 are important for normal retinal function, we took advantage of CaBP1/caldendrin and CaBP2 deficient mice. Although these proteins are not required for retinal development and

maintenance, CaBP1/caldendrin and CaBP2 are important for normal transfer of light signals through the retina.

Introduction.

CaBPs are neuronal Ca^{2+}-binding proteins with high homology to calmodulin (CaM) (Haeseleer et al., 2000). CaBPs possess 4 EF-hand Ca^{2+}-binding domains, but unlike CaM, only 3 of them are capable of binding Ca^{2+}. CaM and CaBPs can interact with similar targets, but their differences can underlie distinct forms of regulation. For example, CaM and CaBPs can both bind to voltage-gated Ca_v1 L-type Ca^{2+} channels, but CaM promotes Ca^{2+}-dependent inactivation while CaBPs oppose this process and prolong channel opening (Zhou et al., 2004; Cui et al., 2007).

CaBPs are expressed in the retina and in the cochlea; CaBP1/caldendrin is also expressed in other neuronal tissues, including the brain (Seidenbecher et al., 1998; Menger et al., 1999; Haeseleer et al., 2000; Haeseleer et al., 2004; Yang et al., 2006; Cui et al., 2007; Kim et al., 2014). CaBP4 has been well-characterized and is essential for normal neurotransmitter release from photoreceptors through enhanced activation of $Ca_v1.4$ L-type channels (Haeseleer et al., 2004; Shaltiel et al., 2012). Mutations in the genes encoding CaBP4 and $Ca_v1.4$ lead to similar visual disorders in humans and animal models (Bech-Hansen et al., 1998; Strom et al., 1998; Boycott et al., 2001; Wutz et al., 2002; Haeseleer et al., 2004; Mansergh et al., 2005; Zeitz et al., 2006; Aldahmesh et al., 2010; Khan et al., 2012; Bijveld et al., 2013; Khan, 2013). CaBP5 is expressed in rod bipolar cells and in type 3 OFF and type 5 ON cone bipolar cells (Haeseleer et al., 2000; Haverkamp et al., 2003a) and is important for normal sensitivity of retinal ganglion cell light responses, likely through regulation of neurotransmitter release (Cui et al., 2007; Rieke et al., 2008; Sokal and Haeseleer, 2011).

CaBP1 and CaBP2 transcripts are alternatively spliced, resulting in short (S-) and long (L-) forms of these proteins (Haeseleer et al., 2000; Sokal et al., 2000; Haeseleer and Palczewski, 2002). A third splice variant of CaBP1, named caldendrin (CD), incorporates a different N-terminal exon and lacks the N-terminal myristoylation site present in the S- and L-CaBP1(Seidenbecher et al., 1998). For simplicity, we will use CaBP1/CD to refer to all three variants (S-CaBP1, L-CaBP1 and caldendrin) and CaBP1 to refer to S-CaBP1 and L-CaBP1. CaBP1/CD is expressed in different regions of the brain and is localized pre- and post-synaptically (Seidenbecher et al., 1998; Kim et al., 2014). In the retina, CaBP1/CD is expressed in OFF cone bipolar cells and in amacrine cells (Menger et al., 1999; Haeseleer et al., 2000; Haverkamp and Wassle, 2000). CaBP1 modulates voltage-gated calcium channels (see (Hardie and Lee, 2016) for review), with different effects on channel activity depending on the subtype of channel (Lee et al., 2002; Zhou et al., 2004; Yang et al., 2006; Cui et al., 2007; Findeisen and Minor, 2010; Few et al., 2011). CaBP1 also regulates inositol 1,4,5-triphosphate receptors (Yang et al., 2002; Haynes et al., 2004; Li et al., 2013) and various enzymes in vitro (Haeseleer et al., 2000; Sokal et al., 2000). Caldendrin interacts with light chain 3 of microtubule-associated protein 1A, A-kinase anchoring proteins 79/150 and the Jacob protein that couples NMDA receptor signaling to the nucleus (Seidenbecher et al., 2004; Dieterich et al., 2008; Gorny et al., 2012). CaBP2 regulates voltage-gated calcium channels, inositol 1,4,5-triphosphate receptors and various enzymes (Haeseleer et al., 2000; Sokal et al., 2000; Yang et al., 2006; Cui et al., 2007). A mutation in the *Cabp2* gene is associated with hearing impairment in humans, likely through dysregulation of the $Ca_v1.3$ channels present in auditory inner hair cells, which are modulated by CaBP2 (Schrauwen et al., 2012).

Despite the identification of a large variety of interacting partners, the contributions of CaBP1/CD and CaBP2 to the transmission of light responses through the retina is unknown. In this study, we used CaBP1/CD knockout (KO) (*Cabp1*$^{-/-}$) and newly generated CaBP2 KO (*Cabp2*$^{-/-}$) mice to investigate the importance of CaBP1/CD and CaBP2 for normal visual function. We find that

both CaBP1/CD and CaBP2 regulate ganglion cell light responses and have different effects on their contrast sensitivity.

Material and methods

Antibodies.

Commercially available antibodies were: Alexa Fluor 555 goat anti-rabbit (Molecular Probes Cat# A21429 RRID:AB_141761), Alexa Fluor 488 goat anti-rabbit (Thermo Fisher Scientific Cat# A11034 RRID:AB_10562715), Alexa Fluor 555 goat anti-rat (Molecular Probes Cat# A21434 RRID:AB_141733), Alexa Fluor 568 goat anti-mouse IgG2a (γ2a)(Innovative Research Cat# A21134 RRID:AB_1500825), Alexa Fluor 488 goat anti-mouse IgG1 (γ1) (Molecular Probes Cat# A21121 RRID:AB_141514), anti-calretinin (Millipore Cat# MAB1568 RRID:AB_94259), anti-synaptotagmin 2 (Zebrafish International Resource Center Cat# znp-1 RRID:AB_10013783), anti-Ctbp2/ribeye (BD Biosciences Cat# 612044 RRID:AB_399431), anti-NK3R (rabbit polyclonal, a kind gift of Dr. Arlene Hirano, UCLA, Los Angeles, CA), anti-GFP (Abcam Cat# ab13970 RRID:AB_300798), anti-calsenilin (Millipore Cat# 05-756 RRID:AB_309969), anti-CaBP1, anti-CaBP2 and anti-CaBP5 (rabbit polyclonal, a kind gift of Françoise Haeseleer, University of Washington, Seattle, WA).

Generation of rat anti-CaBP1/CD and rat anti-CaBP2 antibodies.

Anti- CaBP1/CD and anti-CaBP2 polyclonal antibodies were raised in rats by subcutaneous immunization with purified S-CaBP1 or S-CaBP2 recombinant proteins mixed with Freund's adjuvant (Cocalico Biologicals, Inc., Reamstown, PA). For affinity purification of rat anti-CaBP1/CD or anti-CaBP2 antibodies, purified CaBP1 or CaBP2 were coupled to CNBr-activated Sepharose (GE Health Care, Piscataway, NJ) according to the manufacturer's protocol. After loading of a 10-fold dilution of the sera in PBS, the columns were washed with 20

154 volumes of PBS. The bound antibodies were eluted with 0.1 M glycine buffer, pH 2.5 and
155 dialyzed overnight against PBS.

156 ***Generation and genotyping of Cabp2$^{-/-}$ mice.***

157 All animal procedures were performed in accordance with the [Author University] Animal Care and
158 Use Committee's regulations. A ~ 2.1 kb fragment covering part of exon 2 to part of intron 5 of
159 CaBP2 gene was amplified first from C57Bl/6 genomic DNA by PCR with primer FH939 (5'-
160 GTCGACTAAGTAGCTGAGACCAGAAGAGATCGAAG -3') that was extended with a *SalI*
161 restriction site and includes a Stop codon in all 3 open reading frames and primer FH940 (5'-
162 GGTACCAGGAGGGCTCAGTTGCTCACATTA -3') that was extended with a *KpnI* site. After
163 sequencing of this 2.1 kb fragment, it was cloned into the targeting vector opened *SalI* and *KpnI*
164 between the neomycin phosphotransferase gene and herpes simplex virus thymydine kinase
165 gene. The long arm of ~5.2 kb covering the promoter region of the *Cabp2* gene upstream the
166 ATG was amplified in 2 fragments. The upstream fragment of 2kb was amplified by PCR with
167 primer FH937 (5'- GCGGCCGCTCGTGGTTTCAGGTGCTCTACACA -3') that was extended
168 with a *NotI* site and primer FH947
169 (5'- TAAGGTCTTAGAGGGTCTGACAGG -3') that covers a *SpeI* restriction site. A 3.2 kb
170 fragment upstream of the CaBP2 initiation codon was amplified by PCR with primer FH938 (5'-
171 ACCCAGGTTTCTGGCCTTATGTCT-3') that also covers the *SpeI* restriction site and FH948
172 (5'- TACCGACTGACTCATGCCTAGGTT-3') which hybridizes a few bases downstream the
173 CaBP2 initiation codon. All fragments were cloned in the pCRII-TOPO vector and sequenced. A
174 td-tomato vector (originally a kind gift from Dr. Roger Tsien, kindly provided by Dr. Rachel
175 Wong) was modified by mutagenesis using the QuikChange Lightning Multi Site-Directed
176 Mutagenesis (Agilent technologies) to introduce a *NheI* site after the SV40 polyadenylation site
177 with primer FH1043 (5'-
178 GTATCTTAAGGCGTAGCTAGCAAGCTTTAATATTTTGTTAAAATTCGC-3') and to delete the

internal *NcoI* site in td-tomato with primer FH1044 (5'-CGTAATGCAGAAGAAGACGATGGGCTGGGAGGCCTCC-3'). Td-tomato was then fused to the CaBP2 promoter as a fragment *NcoI-NheI* and transferred together in the targeting vector as *NotI_BglII* and *BglII-NheI* fragments.

The *KpnI* linearized targeting vector was electoporated into B6/BLU embryonic stem cells. Recombinant clones were selected on medium containing G418. Transfected ES cells clones were first screened through PCR analysis. To screen for homologous recombination, we used primers FH 1064 (5'- GGGTCGTTTGTTCGGATCCTCTAGAGTC -3') located in the neo cassette and FH1139 (5'- TACACAGGCTCACCGAGACATCAT-3') hybridizing approximately 163 bp downstream of the 3'end of the short arm in the Cabp2 gene and amplifying a fragment of ~2.3 kb. A control PCR for the wild-type gene was made with primers FH1139 and FH1140 (5'- ACCAGGCATGGAGTTGGGTATGAA-3') hybridizing in intron 2A, 480bp upstream of the 5' end of the short arm of the Cabp2 gene and amplifying a fragment of ~2.75 kb. Targeted disruption of the *Cabp2* gene was then confirmed by Southern blot analysis. Ten micrograms of genomic DNA was digested with *MfeI* and hybridized with a 0.6 kb 5'end probe located 100 bp upstream of the 5'end of the long arm (Fig. 1). This probe hybridized to a *MfeI* fragment of ~ 13.4 kb of the wild-type allele or a *MfeI* fragment of ~9.1 kb if the *Cabp2* gene is targeted.

One targeted ES clone was injected into C57BL/6J blastocysts. One 80% male chimera was crossed with C57BL/6J mice, and agouti offsprings were genotyped by PCR to verify germ line transmission. Confirmation of *Cabp2* gene targeting was first performed with primers FH1139, FH1140 and FH1064 as indicated above. For routine genotyping of the offspring, the wild–type allele was identified with primers FH1214 (5'- CCCTAAGACACCCAGACAGATGA -3', located in intron 2A) and FH1218 (5'- GAAGTGTCAGCCAGATGGACAAA -3', hybridizing in intron 2B) that generate a PCR product of 0.4 kb. The targeted *Cabp2* allele was identified with primers FH1218 and FH1384 (5'- TGGAGAGGCTATTCGGCTATGA-3', located in the *neo* cassette) that produces a PCR product of ~1.07 kb.

RT-PCR analysis of CaBP1 and CaBP2 transcripts.

Total RNAs were isolated from mouse retina using RNeasy kit (Qiagen, Valencia, Ca). Total RNA (1 µg) was subjected to first strand cDNA synthesis using Superscript III reverse transcriptase and oligo(dT) in a volume of 20 µl according to the manufacturer's protocol (Life Technologies Inc, Carlsbad, Ca). Short and long CaBP1 were amplified with common forward FH705 (5'-CACCATGGGCAACTGCGTCAAGTCG-3') and reverse primers FH706 (5'-TCAGCGAGACATCATCCGGACAAAC-3'). Caldendrin was amplified with primers FH1089 (5'-ACACCAATCATATCTGCCGTCTCC-3') and FH1093 (5'-GCGATGGGGAGGAACGGGGGCT-3'). Short and long CaBP2 were amplified with common forward K122 (5'-TCCGGGCCTGGCATGGTTC-3') and reverse FH1410 (5'-CCGAACAAATTCTTCAAAGTCAACC-3'). Amplification of glyceraldehyde 3-phosphate dehydrogenase (GAPDH) with GAPDH F (5'-GAAGGGCTAATGACCACAGTCCAT-3') and GAPDH R (5'-TAGCCATATTCGTTGTCGTACCAGG-3') was used as a positive control. The PCR conditions were as followed: 94°C for 2 min, 35 cycles at 94°C for 15 s, 64°C for 30 s and 72°C for 1 min then 72°C for 7 min.

Immunohistochemistry.

Eyecups from 6-week to 3-month old *Cabp1*$^{-/-}$, *Cabp2*$^{-/-}$, *Cabp1*$^{-/-}$ /*Cabp2*$^{-/-}$ or wild type (WT) mice of either sex were fixed in 4% paraformaldehyde in 0.1 M phosphate buffer, pH 7.4 (PB) for 1 h. After fixation, tissues were immersed in a graded sucrose series to 20% sucrose in 0.1 M phosphate buffer pH7.4 (PB), and then embedded in 33% OCT compound (Miles, Elkhart, NY) diluted with 20% sucrose in PB before being frozen. Eye tissues were cut in 12 µm sections. To block non-specific labeling, retinal sections were incubated with 3% normal goat serum in PBST buffer (10 mM sodium phosphate, 150 mM NaCl, 0.1% Triton X-100, pH 7.4) for 20 min at room temperature. Sections were then incubated overnight at 4˚C with purified rat anti-CaBP1/CD 1:50 dilution or rat anti-CaBP2 1:20 dilution. Alexa Fluor 555-conjugated goat

anti-rat IgG and Hoechst stain (1/2000) were reacted with the sections for 1 hr at room temperature. The sections were rinsed in PBST and mounted with Prolong antifade reagent (Molecular Probes, Oregon). As indicated, some sections were incubated overnight at 4˚C with a mix of rat or rabbit anti- CaBP1/CD or anti-CaBP2 antibodies and rabbit anti-NK3R at 1:500 dilution, mouse anti-Syt2 at 1:200, mouse anti-calretinin at 1:1000, chicken anti-GFP at 1:1000, mouse anti-calsenilin at 1:1000 or rabbit anti-CaBP5 at 1:200. A mix of Alexa Fluor 555-conjugated goat anti-rat IgG (1:400) and Alexa 488-conjugated goat anti-rabbit IgG (1:400), Alexa 488-conjugated goat anti-mouse IgG (1:400) or Alexa 488-conjugated goat anti-chicken IgG (1:400) was then reacted with the sections for 1 hr at room temperature.

For the analysis of wholemount retinas, the mouse retinas were fixed for 1 hour in 4% paraformaldehyde in PB before dissection. The retinas were incubated with 5% normal goat serum in PBST buffer overnight at 4°C. The retinas were then incubated overnight at 4°C with a mix of anti-Syt2 (1:200) or anti-NK3R (1:500) and anti-Ctbp2 (1:1000). After three washes for 15 minutes in PBST, a mix of Alexa Fluor 568 goat anti-mouse IgG2a (γ2a) and Alexa Fluor 488 goat anti-mouse IgG1 (γ1) or a mix of Alexa Fluor 488 goat anti-mouse IgG and Alexa Fluor 555 goat anti-rabbit was then reacted with the sections overnight at 4°C. After three washes in PBST, the retinal wholemounts were mounted with the photoreceptor side down in Prolong antifade reagent and analyzed under a confocal microscope (Zeiss LSM710, Carl Zeiss, NY, USA). Immunofluorescent images were obtained with a 63x/1.4, 40x/1.1 or 40x/1.3 NA (Carl Zeiss, Inc. Thornwood, NY) objectives.

For the quantification of the Ctbp2 labeled synaptic ribbons, confocal images of en face views in wholemounts of WT, *Cabp1*$^{-/-}$ and *Cabp2*$^{-/-}$ retinas were acquired using a 63x1.4 objective at a voxel size of 0.028 X 0.028 X 0.359 um (x-y-z). The sublamina containing the axons terminals of cone OFF bipolar type 1 and type 2 was identified by colabeling with anti-NK3R and anti-Ctbp2. The axon terminals of cone ON bipolar type 6 were visualized by colabeling with anti-syt2 and

Ctbp2. Ctbp2 labeled synaptic ribbons were counted in images of six randomly chosen 25 μm^2 areas across the retina of 4 mice for each phenotype. The statistical analysis was done using the two-tailed Student's t-test. Data are expressed as mean ± s.e.

Electron microscopy.

Eye cups from WT, *Cabp1* $^{-/-}$ and *Cabp2* $^{-/-}$ mice of either sex were fixed in 4% glutaraldehyde in 0.1 M sodium cacodylate buffer at 4°C. After 4 washes in 0.13M phosphate buffer pH7.4 (PB), eyecups were dissected and post fixed in 1% buffered osmium tetroxide, for 2 hours, on ice. After another 4 washes in PB buffer, the retinas were en bloc stained in 1% uranyl acetate overnight at 4°C. The retinas were dehydrated through a graded series of ethanol and two incubations in propylene oxide. Tissue were then infiltrated in a 1:1 mixture of propylene oxide: epon araldite and two incubations in epon araldite, before polymerization at 60°C. Seventy nm sections were cut on a Leica UC7 ultra microtome and stained with Reynolds lead citrate. The sections were viewed and images recorded on a JEOL 1230 electron microscope (JEOL, Peabody, MA). Images of bipolar cells terminals were analyzed in the outer part of the inner plexiform layer within 2 to 5 μm from the inner nuclear layer where type 1 and type 2 cone OFF bipolar cells axon terminals are located. Images of photoreceptor synapses with bipolar cell were taken in the outer plexiform layer.

Electrophysiology and Visual Stimulation.

Experiments were conducted on whole mount retinal preparations taken from dark-adapted wild-type, *Cabp1* $^{-/-}$ or *Cabp2* $^{-/-}$ mice (Schwartz et al., 2012). Isolated retina was stored in oxygenated (95% O_2/5% CO_2) Ames medium (Sigma-Aldrich, St. Louis, MO) at <32°C–34°C. Isolated retinas were flattened onto polyL-lysine slides (whole mount) (Schwartz et al., 2012), placed in a custom microscope, and perfused with Ames solution at a rate of <8 mL/min. Retinal neurons were visualized and targeted for patch-clamp recordings using infrared light (>950 nm). Voltage-clamp recordings were obtained using pipettes (2–3 MΩ) filled with an intracellular solution containing (in

mM): 105 Cs methanesulfonate, 10 TEA-Cl, 20 HEPES, 10 EGTA, 2 QX-314, 5 Mg-ATP, 0.5 Tris-GTP, (<280 mOsm; pH <7.3 with CsOH). Full-field light stimuli (diameter, 500 µm) were delivered to the tissue from an LED with peak spectral output at 405nm. Recordings were performed from ventral retina. All ganglion cell recordings shown were recorded at a background light level of ~900 R*/S cone/sec where cones dominate retinal responses. The statistical analysis was done using the two-tailed unpaired Student's t-test. *p<0.05, **p<0.01, ***p<0.001. Error bars indicate s.d.

Results.

Generation of CaBP2$^{-/-}$ mice. Two splice variants of CaBP2, S-CaBP2 and L-CaBP2, exist and differ by the absence or presence of exon 2A (Fig. 1A, (Seidenbecher et al., 1998; Haeseleer et al., 2000; Sokal et al., 2000)). To generate *CaBP2*$^{-/-}$ mice, we designed a targeting vector to replace exon 1 and exon 2a of the *Cabp2* gene with td-tomato and a PGK-neo cassette as shown in figure 1A. Stop codons were also introduced in all 3 open reading frames of exon 2B to prevent expression of any CaBP2 variants. PCR screening of ES cells identified three targeted ES cell clones for which targeting of the *Cabp2* allele was further verified using Southern blot (Fig. 1B). Injection of targeted ES clone 37 produced 1 male chimera that gave germline transmission. Targeting of the *Cabp2* gene was confirmed in the offspring by PCR on genomic DNA (Fig. 1C). *CaBP2*$^{-/-}$ mice were viable and did not show any apparent physiological deficits or breeding problems.

Analysis of CaBP1/CD and CaBP2 expression in knockout mice.

The generation of *Cabp1* $^{-/-}$ mice was described by Kim et al (Kim et al., 2014). As a first step in the characterization of *Cabp1* $^{-/-}$ mice, we verified the absence of CaBP1/CD expression in the retina. Because exon 1 of caldendrin and exon 1 of S- and L-CaBP1 were removed in *Cabp1* $^{-/-}$ mice, all three splice variants were targeted. The absence of transcripts for all three splice variants

was confirmed by RT-PCR using retinal RNA of *Cabp1* $^{-/-}$ mice (Fig. 2A) while all 3 variants were observed in *Cabp1* $^{+/+}$ mice. As a positive control, PCR were performed with primers designed to detect GAPDH and showed transcripts in both *Cabp1* $^{+/+}$ and *Cabp1* $^{-/-}$ mice. The absence of CaBP1/CD proteins in the retina of *Cabp1* $^{-/-}$ mice (Fig. 2B) was confirmed using immunohistochemistry. Staining was not detected in *Cabp1* $^{-/-}$ mice with anti-CaBP1/CD antibodies recognizing all three splice variants.

We also verified the absence of CaBP2 expression in the newly generated *Cabp2* $^{-/-}$ mice. Using RT-PCR, transcripts were not detected for CaBP2 in *Cabp2* $^{-/-}$ retina (Fig. 2C) that showed transcripts for the GAPDH positive control. Using immunohistochemistry, we tested that CaBP2 proteins are not present in *Cabp2* $^{-/-}$ mice. Unfortunately, because of the high homology between CaBP1/CD and CaBP2 proteins, our anti-CaBP2 antibodies recognize both CaBP1/CD and CaBP2. As a consequence, signals were still observed in the inner nuclear layer of *Cabp2* $^{-/-}$ mouse retina immunolabeled with anti-CaBP2 (Fig. 2D). This residual signal was confirmed to be due to crossreactivity of anti-CaBP2 antibodies with CaBP1/CD proteins as demonstrated by the absence of signals in *Cabp1* $^{-/-}$/ *Cabp2* $^{-/-}$ double KO retinas immunolabeled with anti-CaBP2 (Fig. 2D). Therefore, specific labeling of CaBP2 proteins can be visualized with our anti-CaBP2 antibodies in *Cabp1* $^{-/-}$ mouse retina. All together, these results confirmed that CaBP1/CD and CaBP2 are not expressed in *Cabp1* $^{-/-}$ and *Cabp2* $^{-/-}$ mice.

Analysis of retinal morphology in Cabp1 $^{-/-}$ ***mice***.

CaBP1/CD is expressed in the inner retina, specifically in amacrine cells and in OFF cone bipolar cells (Fig. 3, Table 1, (Menger et al., 1999; Haeseleer et al., 2000; Haverkamp and Wassle, 2000; Haverkamp et al., 2003b)). Some CaBP1/CD staining can also be observed in cells in the ganglion cell layer (GCL) that may be displaced amacrine cells (Menger et al., 1999). As shown in figure 3 A, all cells labeled with anti-neurokinin receptor 3 (NK3R), which labels type

1 and type 2 OFF cone bipolar cells, were also labeled with anti-CaBP1/CD (Haverkamp et al., 2003b; Pignatelli and Strettoi, 2004). Synaptotagmin 2 (Syt2), another label for type 2 OFF cone bipolar cells (Wassle et al., 2009), colocalized with CaBP1/CD in the outer IPL (Fig. 3C). Some amacrine cells labeled with anti-calretinin antibodies were also immunostained with anti-CaBP1/CD (Fig. 3B).

To determine if the absence of CaBP1/CD triggers structural changes of the retina, we analyzed the morphology of the retinal cells lacking CaBP1/CD using antibodies against these marker proteins. NK3R and Syt2 immunolabeling showed normal bipolar cell morphology and normal thickness of the INL and IPL in *Cabp1* $^{-/-}$ compared with *Cabp1* $^{+/+}$ retina (Fig. 3D,F). Calretinin immunostaining demonstrated normal stratification of the IPL of *Cabp1* $^{-/-}$ retina (Fig. 3E). To investigate if lack of CaBP1/CD results in synaptic alterations, we analyzed retina colabeled with anti-Syt2 or anti-NK3R and anti- ribeye/CtBP2 that labels synaptic ribbons both in the inner plexiform layer (IPL) and in the outer plexiform layer (OPL). We analyzed the synapses in both plexiform layers because CaBP1/CD is expressed throughout the cone bipolar cells. Normal horseshoe-shaped and punctuate staining of the synaptic ribbons was observed in the IPL (Fig. 4A) and OPL (Fig. 4C) of *Cabp1*$^{-+/+}$ and *Cabp1* $^{-/-}$ mouse retina. We quantified the synaptic ribbons labeled with anti-Ctbp2 in 25 μm^2 fields of the OPL and IPL of WT and *Cabp1* $^{-/-}$ mice. The density of synaptic ribbons in WT and *Cabp1* $^{-/-}$ *mice* did not differ significantly (Table 2). Synaptic terminals were analyzed at higher magnification using transmission electron microscopy to look for more subtle changes. Cone synapse morphology was normal, showing invagination of a pair of horizontal cells and a cone ON bipolar cell (Fig. 4D). Normal membrane anchored synaptic ribbons and tethered vesicles were observed both in the IPL and OPL of *Cabp1*$^{+/+}$ and *Cabp1*$^{-/-}$ retina (Fig. 4B,D). These results suggest that CaBP1/CD is not required for normal development or maintenance of overall retinal morphology.

CaBP2 localization in bipolar cells of the retina.

To determine the consequences of CaBP2 deficiency, we first determined the distribution of CaBP2 in the mouse inner retina. Because our anti-CaBP2 antibody reacts with both CaBP1/CD and CaBP2 (Fig. 2D), and because there are no retina morphological changes in *Cabp1* $^{-/-}$, we chose to study CaBP2 localization using *Cabp1* $^{-/-}$ mouse retina. Anti-CaBP2 labeled axons ramifying in two distinct layers of the IPL, likely corresponding to ON and OFF cone bipolar cells (Fig. 2D). To determine the bipolar cell types that express CaBP2, we used antibodies against selective markers. Double labeling experiments with antibodies against CaBP2 and CaBP5 (Fig. 5A, B, C) demonstrated that CaBP2 does not localize in bipolar cells expressing CaBP5, indicating that CaBP2 is not expressed in type 3 OFF, type 5 ON and rod bipolar cells (Haeseleer et al., 2000; Ghosh et al., 2004). CaBP2 is also not expressed in anti-calsenilin labeled type 4 OFF cone bipolar cells (Fig. 5D, E, F) (Haverkamp et al., 2008). Gustducin-GFP mice express GFP in type 7 ON cone bipolar cells (Lin and Masland, 2005). Although our anti-CaBP2 antibody would crossreact with CaBP1/CD in gustducin-GFP retinas, none of the GFP-labeled cells in these mice were labeled with anti-CaBP2 (Fig. 5G, H, I). We can thus conclude that type 7 ON bipolar cells do not express CaBP1 and CaBP2 proteins.

To visualize the sublaminae of the inner plexiform layer, we labeled the mouse retina with an antibody to calretinin that displays a laminar pattern in three layers of the IPL separating sublaminae 1/2, 2/3, and 3/4 (Wassle, 2004) (Fig. 6C) . Colabeling with anti-CaBP2 and anti-calretinin revealed that CaBP2 localizes in cells with axons in sublamina 1 and in sublamina 3/4 (Fig. 6C). A partial overlap of the distribution of CaBP2 with NK3R indicated that either type 1 or type 2 OFF bipolar cells express CaBP2 (Fig. 6A). Costaining with anti-Syt2 and anti-CaBP2 antibodies showed colocalization of Syt 2 and CaBP2 in sublaminae 3/4 but not in sublamina 1 (Fig. 6B). This result indicates that CaBP2 is expressed in type 6 ON bipolar cells. We can also

conclude from Syt 2 and NK3R labeling experiments that type 1 OFF bipolar cells express CaBP2 (Table 1). Although CaBP2 showed colocalization with Syt2 in sublamina 3/4, additional CaBP2 labeled cells appeared to have their axon arborization extending in sublamina 3/4. Because of the lack of other markers for these bipolar cells, it was not to identify these CaBP2 expressing cells.

Analysis of retinal morphology in Cabp2$^{-/-}$ mice.

To determine if CaBP2 is necessary for normal retinal development and structure, we analyzed the morphology of the CaBP2 deficient cells using antibodies against Syt 2 and NK3R to look at type 6 ON and type 1 OFF bipolar cells. Overall morphology of these bipolar cells and thickness of the retinal layers did not differ noticeably between *Cabp2*$^{+/+}$ and *Cabp2*$^{-/-}$ retina (Fig. 6). The Syt2-labeled axons of type 6 ON bipolar cells in the inner IPL and NK3R-labeled axons of OFF bipolar cells in the outer IPL showed normal morphology (Fig. 7). No difference was observed in the OPL between the Syt2-labeled dendrites of *Cabp2*$^{+/+}$ and *Cabp2*$^{-/-}$ retina. There were also no apparent changes in the number of synapses visualized with anti-Ctbp2 in *Cabp2*$^{-/-}$ mice (Table 2). Normal synaptic ribbons and tethered vesicles were observed both in the IPL and OPL of *Cabp2*$^{+/+}$ and *Cabp2*$^{-/-}$ retina using electron microscopy (Fig. 7B, 7D). Cone bipolar cells and horizontal cells invaginations appeared to make a normal synapse with cone photoreceptors (Fig. 7D).

Altered light responses of ganglion cells in Cabp1$^{-/-}$ and Cabp2$^{-/-}$ mice.

To determine if CaBP1/CD and CaBP2 are important for retinal function, we measured ganglion cell responses to full-field light stimuli. We selected three well-characterized mouse ganglion cell types – On-alpha, OFF transient (OFF T) and OFF sustained (OFF S). Extensive work on these alpha-like ganglion cells has identified type-specific response properties generated from distinct circuit mechanisms (Pang et al., 2003; Murphy and Rieke, 2006; van Wyk et al., 2009; Schwartz

et al., 2012). Recordings were performed at a background of 900 R*/Scone/sec where cones dominate retinal responses.

Since CaBP2 is expressed in Type 6 bipolar cells and ON alpha ganglion cells receive most excitatory synaptic input from this bipolar cell type (Morgan et al., 2011; Schwartz et al., 2012), we chose ON alphas as the primary candidate for studying perturbation in ganglion cell function in *Cabp2*$^{-/-}$ retinas (Fig. 8). Responses to a 100% contrast light flash were significantly smaller in mice lacking CaBP2 (Fig. 8C-D).

We characterized the response kinetics and contrast sensitivity using linear-nonlinear (LN) models computed from excitatory synaptic currents in response to a random noise stimulus (Chichilnisky, 2001; Kim and Rieke, 2001; Rieke, 2001). This model provides a relatively simple description of how continuous light inputs are transformed into cellular responses and provides an effective means of characterizing contrast-dependent changes in the amplitude and kinetics of the light response of a cell. The model consists of a linear filter that accounts for the time course of the response and a time-independent or "static" nonlinearity that converts the filtered stimulus into responses (excitatory synaptic currents; Fig. 8).

The linear filters of ON alpha ganglion cells were slightly slower in *Cabp2*$^{-/-}$ retinas compared to control retinas (Fig. 8F-G). The nonlinearities were strikingly different between the ON alpha ganglion cells of *Cabp2*$^{+/+}$ and *Cabp2*$^{-/-}$ retinas (Fig. 8H-I).

The response range of the responses – i.e. the difference between the maximum and minimum excitatory synaptic current evoked by the random noise stimulus -- was significantly smaller for ON alpha ganglion cells in *Cabp2*$^{-/-}$ retinas compared to control cells (Fig. 8H-I).

Since CaBP1/CD is expressed in OFF bipolar cells, we analyzed responses of OFF S and OFF T ganglion cells in *Cabp1*$^{-/-}$ retinas. Differences in lamination of OFF S and OFF T ganglion cells in the inner plexiform player suggest that they derive their excitatory inputs from different OFF bipolar cells. Responses to a light flash were larger and slower for OFF T ganglion cells

compared to control retinas. Responses of OFF S ganglion cells in *Cabp1*$^{-/-}$ retinas to a light flash exhibited no significant difference in amplitude with respect to the control retinas (Fig. 9A-B). The response kinetics were slower for OFF S and OFF T ganglion cells in *Cabp1*$^{-/-}$ retinas compared to controls (Fig. 9A-B). Nonlinearities were strikingly different between the OFF alpha ganglion cells from *Cabp1*$^{-/-}$ and control retinas (Fig. 9A-B). The change in the nonlinearity was opposite for OFF S and OFF T ganglion cells, with a smaller response range for *Cabp1*$^{-/-}$ OFF S ganglion cells and larger response range for *Cabp1*$^{-/-}$ OFF T ganglion cells. Changes in excitatory synaptic currents affect the spike output of the ganglion cells. Indeed spike responses of ON alpha ganglion cell to a 100% contrast step were weaker in *Cabp2*$^{-/-}$ retinas than in control retinas (Fig. 10). Similarly, OFF T ganglion cells exhibited a stronger spike response in *Cabp1*$^{-/-}$ than in control retinas (Fig. 10).

We also compared excitatory synaptic currents of ON alpha ganglion cells in *Cabp1*$^{-/-}$ retinas and of OFF T ganglion cells in *Cabp2*$^{-/-}$ retinas with corresponding control cells (Fig. 11). Responses of these cells could be affected since CaBP1/CD is expressed in amacrine cells and CaBP2 is expressed in Type 1 OFF bipolar cells. Interestingly, the response kinetics of the ON alpha ganglion cells were slower but the response range was unchanged or slightly increased in *Cabp1*$^{-/-}$ retinas, unlike in *Cabp2*$^{-/-}$ retinas (Fig. 11). The response kinetics of the OFF T ganglion cells and the response range of responses did not change significantly in *Cabp2*$^{-/-}$ retinas (Fig. 11).

Discussion.

Ca^{2+}-binding proteins modulate the cellular activities of enzymes, channels and structural proteins in response to changes in intracellular [Ca^{2+}]. Here, we determined if the lack of CaBP1/CD or CaBP2, neuronal calcium binding proteins expressed in distinct retinal secondary neurons, results in altered transmission of light responses through the retina. We found that not

455 only the kinetics but also the amplitude and response range of the light responses in ganglion
456 cells are affected in the absence of CaBP1/CD or CaBP2, while the overall morphology of the
457 CaBP1/CD or CaBP2 deficient retina and synapses is not affected. These findings give a first
458 insight into the importance of CaBP1/CD and CaBP2 for normal visual function.
459

460 **CaBP2 is expressed in cone ON and OFF bipolar cells.**

461 Our immunohistochemistry results showed that CaBP2 is expressed in type 1 cone OFF bipolar
462 and type 6 cone ON bipolar cells. Type 1 cone ON bipolar cells are the first retinal neurons to
463 date shown to express two different CaBPs, CaBP2 and CaBP1/CD (fig. 3, 6 (Haverkamp et al.,
464 2003b)) since CaBPs were previously shown to be expressed in distinct neurons (Haeseleer et
465 al., 2000; Haverkamp et al., 2003b; Ghosh et al., 2004; Haeseleer et al., 2004). This raises the
466 question of whether CaBP1/CD and CaBP2 might modulate different targets and/or have a
467 different effect on the same target in type 1 cone OFF bipolar cells. In addition to type 1 and
468 type 6 cone bipolar cells, other cells of the inner nuclear layers in sublamina 3/4 appeared to be
469 immunostained with anti-CaBP2 antibody. Although we cannot exclude that type 8 and type 9
470 bipolar cells might express CaBP2, the axons of those cell types have been described to stratify in
471 S4, S5 (Ghosh et al., 2004) rather than S3,S4 as observed for the CaBP2 labeled cells. Still, type
472 8 bipolar cells appeared to stratify broadly with the Syt2 labeled type 6 bipolar cells (Dunn and
473 Wong, 2012). These unidentified CaBP2 labeled cells looked rather similar to the previously
474 CB3,4 cells visualized using gene gun labeling and displaying a broad axonal arbor that extends
475 through layers 3 and 4 (Pignatelli and Strettoi, 2004).

476 **Retinal morphology of *Cabp1* $^{-/-}$ and *Cabp2* $^{-/-}$ mice is normal.**

477 Immunohistochemistry analysis of *Cabp1* $^{-/-}$ and *Cabp2* $^{-/-}$ mouse retina using specific markers
478 showed no changes in the cell, dendritic and axon morphologies of cells deficient for CaBP1/CD

or CaBP2. Analysis of synapses by immunostaining with Ctbp2 or by electron microscopy did not reveal changes in the morphology or density of synaptic ribbons or tethered synaptic vesicles. This suggests that CaBP1/CD and CaBP2 are not essential for the development and maintenance of a normal synapse and for the docking of synaptic vesicles. Similar results were obtained for CaBP5 knockout mice. As for *Cabp1* $^{-/-}$ and *Cabp2* $^{-/-}$ mouse retina, no significant changes in the number of synaptic vesicles or docked synaptic vesicles was observed in *Cabp5* $^{-/-}$ mouse retina (Rieke et al., 2008). However, CaBP5 was shown to stimulate synaptic vesicle exocytosis (Sokal and Haeseleer, 2011). It is thus possible that CaBP1/CD and CaBP2 might play a role in neurotransmitter release by regulating events beyond vesicles docking.

Kinetics and amplitude of ganglion cells responses are affected in *Cabp1* $^{-/-}$ and *Cabp2* $^{-/-}$ mice.

We investigated the light responses of alpha ganglion cells to determine the importance of CaBP1/CD and CaBP2 for proper transmission of light responses across the retina. Compared with responses of ganglion cells from wild type retina, we observed a ~ 50 % increase in the amplitude of the excitatory postsynaptic currents of OFF T ganglion cells of *Cabp1*$^{-/-}$ mice and a ~ 60% decrease of the excitatory synaptic currents in ON-alpha ganglion cells of *Cabp2*$^{-/-}$ mice. Since CaBP1/CD and CaBP2 are expressed throughout bipolar cells, it is possible that these altered responses originate from a defect in the processing of the light signal received from cones. Such defect at the cone to cone bipolar cell synapse should affect the electroretinograms of *Cabp1*$^{-/-}$ and *Cabp2*$^{-/-}$ mice. However, the time to peak and amplitude of b-waves of electroretinograms of *Cabp1*$^{-/-}$ and *Cabp2*$^{-/-}$ mice did not differ significantly from electroretinograms from wild type mice (data not shown); this suggests that alterations in the transmission of the light signal occur likely downstream of the bipolar cell dendrites. Interestingly, the two OFF-alpha ganglion cell types displayed similar changes in kinetics but opposite changes in response range in *Cabp1*$^{-/-}$ mice. The opposite changes in response range

could be explained if the bipolar cells that provide input to OFF S and OFF T ganglion cells express different targets for CaBP1/CD. Alternatively, CaBP1 may shape the synaptic input to these two types of OFF ganglions cells differently.

The absence of CaBP2 resulted in a decrease in the response range of the ON alpha ganglion cell response. The absence of CaBP1/CD slowed response kinetics but did not change the response range of the excitatory synaptic currents of the ON-alpha ganglion cells. Since CaBP1 is not found in cone ON bipolar cells, the effect of CaBP1 deficiency on ON-alpha ganglion cell excitatory inputs could result from alterations in responses of amacrine cells that provide presynaptic inhibition on type 6 bipolar cells and shape the kinetics of excitatory inputs of ON-alpha ganglion cells. The complex interplay between ON and OFF pathways means that other explanations are possible as well.

While CaBP2 deficiency results in decreased amplitude of the excitatory synaptic currents in ON alpha ganglion cells (Fig. 8), the lack of CaBP1/CD causes an increase of OFF ganglion cell responses (Fig.9). This opposite effect on the amplitude of ganglion cell responses suggests that CaBPs may have different targets in different cell types or opposing effects on similar targets. Prominent targets of CaBPs, including CaBP1 and CaBP2, are the voltage-gated Ca^{2+} channels (Lee et al., 2002; Haeseleer et al., 2004; Zhou et al., 2004; Cui et al., 2007; Rieke et al., 2008; Schrauwen et al., 2012). Voltage-gated Ca^{2+} channels are directly involved in vesicle exocytosis and are a possible target for CaBP1/CD and CaBP2 in bipolar cells and amacrine cells (Pan et al., 2001; Habermann et al., 2003; Singer and Diamond, 2003; Balakrishnan et al., 2015). Specifically for CaBP1, it was shown that CaBP1 has opposite effects depending on the type of voltage-gated Ca^{2+} channels it modulates (Haeseleer et al., 2000; Lee et al., 2002; Zhou et al., 2004; Cui et al., 2007). Since CaBPs can both inhibit or activate voltage-gated calcium channels, it might concomitantly decrease or increase synaptic vesicle release. Using

electrophysiological recordings, cone bipolar cells have been shown to express diverse Ca_v channels, including Ca_v1 (L-type) and Ca_v3 (T-type) (Kaneko et al., 1989; Pan, 2000; Pan et al., 2001). T-type Ca^{2+} channels have not been shown to be modulated by calmodulin or calmodulin-like CaBPs. Although CaBP1 can interact directly with L-type and P/Q type calcium channels (Lee et al., 2002; Zhou et al., 2004; Cui et al., 2007), it could also modulate Ca^{2+} channel activity by protein kinase pathways. Indeed, in vitro experiments have shown that CaBP1 and CaBP2 can modulate calmodulin kinase II (CaMKII) activity (Haeseleer et al., 2000) and CaMKII promotes the activity of T-type voltage-gated calcium channels (Welsby et al., 2003). The variety of voltage-gated calcium channels expressed in the inner retinal neurons and their specific regulation by CaBPs might thus account for the distinct effect of CaBP1/CD and CaBP2 deficiency on the transmission of light responses to ganglion cells.

CaBPs have also been shown to interact with other proteins playing an important role in neurotransmitter release. For example, CaBP5 interacts with Munc 18-1, a component of the synaptic vesicle cycle. CaBP5 was suggested to have a role in synaptic vesicle priming by binding to a specific domain of Munc18-1 necessary for its interaction with the soluble N-ethylmaleimide-sensitive fusion protein attachment protein receptors (SNARE) complex. We found here that deficiency of CaBP1/CD also results in slower response kinetics than in wild-type animals. If CaBP1/CD would have similar effects on synaptic vesicles priming, it could affect the kinetic of the light responses.

In conclusion, the phenotype of *Cabp1* $^{-/-}$ and *Cabp2* $^{-/-}$ mice gives us a first insight into the important role of CaBP1/CD and CaBP2 for normal transmission of the light responses through retinal circuits. Although the effects of CaBP1/CD and CaBP2 deficiency might result from a change of modulation of voltage-gated calcium channels, other cellular processes might also be altered. Future experiments investigating the interacting partners for CaBP1/CD and CaBP2 in

554 bipolar cells will help to explain the visual phenotypes in the CaBPs knockout mice and the
555 cellular functions of these proteins in the retina.

556 **Figure legends**

557 **Figure 1. Targeting of the *Cabp2* gene. A. Scheme of the mouse *Cabp2* gene with its**
558 **exons.** Arrows above the scheme indicate primers used to clone by PCR *Cabp2* genomic
559 fragments. The *PGK-DTA* and *HSV-TK* cassettes were included in the targeting vector for
560 negative selection in transfected ES cells. In the targeting vector, the *neo* cassette (positive
561 selection) replaces exon 1 and exon 2A of the *Cabp2* gene. The targeting vector is constructed
562 by using a ~5 kb DNA fragment as long arm that extends upstream of the initial ATG and covers
563 the CaBP2 promoter. TdTomato was cloned and fused on the initiation codon of CaBP2. The
564 short arm is a ~2.0 kb genomic fragment encompassing exon 2B to intron 5 of the *Cabp2* gene.
565 Arrows (FH1064, FH1139 and Fh1140) below the scheme indicate primers used to select
566 targeted *Cabp2* allele. The location of *MfeI* restriction site as well as the probe (probe SB) used
567 for analysis of the targeted allele using Southern blot are also indicated. **B. Southern blot**
568 **analysis of ES cell clones.** *MfeI*-digested genomic DNA isolated from wild-type B6/Blu ES
569 cells (WT), or targeted clones 1, 37 and 40 was analyzed by Southern blot with an external
570 probe as shown in A and shows a fragment of 13.4 kb for the wild-type *Cabp2* allele and a
571 fragment of 9.1 kb for the targeted *Cabp2* allele. **C. PCR-based analysis of mice for *Cabp2***
572 **targeting.** A 2.3 kb and 2.75 kb PCR product is amplified with primers FH1140 and FH1139 as
573 shown in A for the wild-type *Cabp2* allele and with primers FH1064 and FH1139 for the targeted
574 allele, respectively.

575 **Figure 2. Analysis of the expression of CaBP1/CD or CaBP2 in wild-type and *Cabp1*$^{-/-}$ or**
576 ***Cabp2*$^{-/-}$ mice, respectively. A. PCR analysis of CaBP1 and caldendrin transcripts.** PCR
577 amplification of both S-CaBP1/L-CaBP1 variants or caldendrin using RNA from *Cabp1*$^{+/+}$ or

Cabp1$^{-/-}$ mouse retina. PCR amplification in the absence of DNA (-) was used as a negative control and amplification of GAPDH was the positive control. **B. Analysis of CaBP1/CD proteins using immunohistochemistry.** Immunolocalization of CaBP1/CD in the retina of 2-month old *Cabp1*$^{+/+}$ and *Cabp1*$^{-/-}$ mice using rat anti-CaBP1/CD antibodies. Nuclei are labeled with Hoechst. Lack of CaBP1/CD immunoreactivity confirms targeting of the *Cabp1* gene. Scale bar: 20 μm. **C. PCR analysis of CaBP2 transcripts.** PCR amplification of both S-CaBP2/L-CaBP2 variants from *Cabp2*$^{+/+}$ or *Cabp2*$^{-/-}$ mouse retina. Controls as described in A. **D. Analysis of CaBP2 proteins using immunohistochemistry.** Immunolocalization of CaBP2 in the retina of 2-month old *Cabp2*$^{+/+}$, *Cabp2*$^{-/-}$, *Cabp1*$^{-/-}$ and *Cabp1*$^{-/-}$ /*Cabp2*$^{-/-}$ mice using rat anti-CaBP2 antibodies. Nuclei are labeled with Hoechst. Crossreactivity of anti-CaBP2 antibody is revealed by labeling of *Cabp2*$^{-/-}$ mouse retina with this antibody and results in staining signals in the inner retina of *Cabp2*$^{-/-}$ retina. The absence of staining in *Cabp1*$^{-/-}$ /*Cabp2*$^{-/-}$ double KO mice demonstrates that the crossreactivity of anti-CaBP2 antibodies is against the CaBP1/CD proteins. Specific labeling of CaBP2 in the inner retina is revealed by labeling of *Cabp1*$^{-/-}$ mouse retina with anti-CaBP2 antibodies. Scale bar: 20 μm.

Figure 3. Analysis of the CaBP1/CD-expressing cells in *Cabp1*$^{+/+}$ and *Cabp1*$^{-/-}$ mice. A. CaBP1/CD localizes in cells expressing NK3R in the inner retina. Analysis of *Cabp1*$^{+/+}$ mouse retina labeled with anti-NK3R (green) and rat anti-CaBP1/CD (red) using confocal microscopy. All cells labeled anti-NK3R labeled are also stained with anti-CaBP1/CD. Arrows in the right panels point to some of the yellow colocalization signals. INL: inner nuclear layer, IPL: inner plexiform layer, GCL: ganglion cell layer. **B. CaBP1/CD localizes in many cells expressing calretinin in the inner retina of *Cabp1*$^{+/+}$ mouse retina.** Legend as in A with anti-calretinin (green). **C. CaBP1/CD colocalizes with synaptotagmin 2 in the outer IPL.** Legend as in A with anti-Syt2 (green). **D to F. Morphology of CaBP1/CD-deficient cells (NK3R**

602 **stained type 1 and 2 bipolar cells, calretinin-stained amacrine cells and Syt2-stained type**
603 **2 bipolar cells) is normal in *Cabp1*$^{-/-}$ mouse retina. A to F.** Scale Bar: 10 μm.
604
605 **Figure 4. Ribbon synapse morphology in the OPL and IPL of *Cabp1*$^{+/+}$ and *Cabp1*$^{-/-}$ mice.**
606 **A.** Confocal images showing en face views of the axon terminals of Syt2-labeled type 2 cone
607 OFF bipolar cells (selected in IPL outer sublamina) or NK3R-labeled type 1 and 2 cone OFF
608 bipolar cells in *Cabp1*$^{+/+}$ and *Cabp1*$^{-/-}$ retina wholemounts. Synaptic ribbons were visualized
609 with anti-Ctbp2 (green). The axons and ribbons appear normal in both *Cabp1*$^{+/+}$ and *Cabp1*$^{-/-}$
610 retina. Scale bar: 2 μm. **B.** Representative electron micrographs of cone OFF bipolar cells in
611 mouse retina cross-sections through the IPL within 5 μm from the inner nuclear layer. Normal
612 ribbons and tethered vesicles are observed both in *Cabp1*$^{+/+}$ and *Cabp1*$^{-/-}$ *retina.* Scale bar:
613 200 nm. **C.** En face views of the dendrites of type 2 cone OFF and type 6 cone ON bipolar cells
614 in the OPL of mouse retina wholemounts labeled with anti-Syt2 (red) and anti-Ctbp2 (green).
615 Scale bar: 2 μm. **D.** Representative electron micrographs of mouse retina cross-sections
616 through the OPL. Scale bar: 200 nm.
617
618 **Figure 5. Immunolocalization of CaBP2 in mouse retina.** Confocal images of *Cabp1*$^{-/-}$ (A - F)
619 or Gus-GFP (G - I) mouse retina double labeled for CaBP2 and CaBP5 (A – C), Calsenilin (D –
620 F) and GFP (G - I). Sublaminae 1 to 5 are indicated in panel C. Scale bar: 10 μm.

621 **Figure 6. Analysis of the CaBP2-expressing cells in *Cabp2*$^{+/+}$ and *Cabp2*$^{-/-}$ mice. A. CaBP2**
622 **localizes in some cells expressing NK3R in the inner retina.** Analysis of *Cabp2*$^{+/+}$ mouse
623 retina labeled with anti-NK3R (green) and rat anti-CaBP2 (red) using confocal microscopy.
624 Some cells labeled anti-NK3R labeled are also stained with anti-CaBP2. Arrows in the right
625 panels point to some of the yellow colocalization signals. INL: inner nuclear layer, IPL: inner
626 plexiform layer, GCL: ganglion cell layer. **B. CaBP2 localizes in some cells expressing**

synaptotagmin 2 in the inner retina of *Cabp2*$^{+/+}$ mouse retina. Legend as in A with anti-Syt2 (green). The area shown at higher magnification in the bottom panels is indicated by the white box. **C. CaBP2 labeled cells terminate their axons in sublamina 1 and in sublamina 3/4.** Legend as in A with anti-calretinin (green). Sublaminae 1 to 5 are indicated in the right panel. **D to F. The overall morphology of the retina and CaBP2-deficient cells (NK3R and synaptotagmin labeled bipolar cells) is normal in *Cabp2*$^{-/-}$ mouse retina.**

Figure 7. Ribbon synapse morphology in the OPL and IPL of *Cabp2*$^{+/+}$ and *Cabp2*$^{-/-}$ mice. **A.** Confocal images of en face views of the axon terminals of Syt2-labeled type 6 cone ON bipolar cells (selected in IPL inner lamina) or NK3R-labeled cone OFF bipolar cells in *Cabp2*$^{+/+}$ and *Cabp2*$^{-/-}$ retina wholemounts. Synaptic ribbons were visualized with anti-Ctbp2 (green). The axons and ribbons of *Cabp2*$^{+/+}$ and *Cabp2*$^{-/-}$ retina appear similar. Scale bar: 2 μm. **B.** Representative electron micrographs of cone OFF bipolar cells in mouse retina cross-sections through the IPL within 2 μm from the inner nuclear layer. Scale bar: 200 nm. **C.** En face views of the dendrites of type 2 cone OFF and type 6 cone ON bipolar cells in the OPL of mouse retina wholemounts labeled with anti-Syt2 (red) or anti-Ctbp2 (green). Scale bar: 2 μm. **D.** Representative of electron micrographs of cone terminals in mouse retina cross-sections through the OPL. Scale bar: 200 nm.

Figure 8. ON alpha ganglion cell responses in *Cabp2*$^{+/+}$ and *Cabp2*$^{-/-}$ mice.

A. Maximum projection image of an exemplar ON alpha ganglion cell filled with dye post-recording. **B.** Exemplar spike raster from an ON alpha ganglion cell in response to 100% contrast step. **C.** Average excitatory synaptic currents in response to 10 ms flash of 100% contrast. **D.** Bar graph comparing the peak amplitude of synaptic response shown in **C** across all cells between control and *Cabp2*$^{-/-}$. **E.** Linear-nonlinear (LN) model - a time-varying random

652 stimulus and the resulting ganglion cell excitatory synaptic inputs were used to derive the linear
653 filter and static nonlinearity that relate the stimulus to the response (top). **F.** Average
654 normalized linear filters for the stimuli. **G.** Quantification of the time to peak i.e. latency of the
655 peaks in linear filters. **H.** Nonlinearities of ganglion cells for the noise stimuli**. I.** Quantification of
656 the response range of the measured response across all cells.

657

658 **Figure 9. OFF alpha ganglion cell responses in *Cabp1*$^{+/+}$ and *Cabp1*$^{-/-}$ mice.**

659 **A-B (i).** Maximum projection image of an exemplar OFF sustained and OFF transient alpha
660 ganglion cell filled with dye post-recording. **A-B (ii).** Exemplar spike raster in response to 100%
661 contrast step. **A-B (iii).** Average excitatory synaptic currents in response to a 10 ms flash of
662 100% contrast from control and *Cabp1*$^{-/-}$retinas. **A-B (iv).** Quantification of the peak amplitude
663 of synaptic response shown in (iii) across all cells between control and *Cabp1*$^{-/-}$ retinas. **A-B (v).**
664 Linear-nonlinear (LN) model - average normalized linear filters for the stimuli. **A-B (vi).**
665 Quantification of the time to peak i.e. latency of the peaks in linear filters. **A-B (vii).** Average
666 nonlinearities of ganglion cells for the noise stimuli**. A-B (viii).** Quantification of the response
667 range of the measured response across all cells between control and *Cabp1*$^{-/-}$ retinas.

668

669 **Figure 10. Spike responses of ON and OFF alpha ganglion cells in control, *Cabp1*$^{-/-}$ and**
670 ***Cabp2*$^{-/-}$ mice. A.** Average peri-stimulus histogram of a spike response to a 100% contrast step
671 in ON alpha ganglion cells in *Cabp2*$^{+/+}$ and *Cabp2*$^{-/-}$ retinas. **B.** Quantification of the peak spike
672 rate shown in A. **C.** Average peri-stimulus histogram of a spike response to a 100% contrast
673 step in OFF transient ganglion cells in *Cabp1*$^{+/+}$ and *Cabp1*$^{-/-}$ retinas. **D.** Quantification of the
674 peak spike rate shown in C.

675

676 **Figure 11. ON and OFF alpha ganglion cell responses in control, *Cabp1*$^{-/-}$ and *Cabp2*$^{-/-}$**
677 **mice.** Linear-nonlinear (LN) model; **A-B.** Average normalized linear filters and quantification of
678 the time to peak i.e. latency of the peaks in linear filters in *Cabp1*$^{-/-}$ and control retinas of ON
679 alpha GC. **C.** Average nonlinearities of ON alpha ganglion cells for the noise stimuli. **D.**
680 Quantification of the response range of the measured response across all ON alpha GC cells in
681 *Cabp1*$^{-/-}$ and control retinas. **E-F.** Average normalized linear filters and quantification of the time
682 to peak i.e. latency of the peaks in linear filters in *Cabp2*$^{-/-}$ and control retinas of OFF transient
683 GC. **G.** Average nonlinearities of OFF transient ganglion cells for the noise stimuli. **H.**
684 Quantification of the response range of the measured response across all OFF transient GC
685 cells in *Cabp2*$^{-/-}$ and control retinas.

686

687 **References**

688 Aldahmesh MA, Al-Owain M, Alqahtani F, Hazzaa S, Alkuraya FS (2010) A null mutation in
689 CABP4 causes Leber's congenital amaurosis-like phenotype. Molecular Vision 16:207-
690 212.
691 Balakrishnan V, Puthussery T, Kim MH, Taylor WR, von Gersdorff H (2015) Synaptic Vesicle
692 Exocytosis at the Dendritic Lobules of an Inhibitory Interneuron in the Mammalian
693 Retina. Neuron 87:563-575.
694 Bech-Hansen NT, Naylor MJ, Maybaum TA, Pearce WG, Koop B, Fishman GA, Mets M,
695 Musarella MA, Boycott KM (1998) Loss-of-function mutations in a calcium-channel
696 alpha(1)-subunit gene in Xp11.23 cause incomplete X-linked congenital stationary night
697 blindness. Nature Genetics 19:264-267.
698 Bijveld MM, Florijn RJ, Bergen AA, van den Born LI, Kamermans M, Prick L, Riemslag FC, van
699 Schooneveld MJ, Kappers AM, van Genderen MM (2013) Genotype and phenotype of
700 101 dutch patients with congenital stationary night blindness. Ophthalmology 120:2072-
701 2081.
702 Boycott KM, Maybaum TA, Naylor MJ, Weleber RG, Robitaille J, Miyake Y, Bergen AA, Pierpont
703 ME, Pearce WG, Bech-Hansen NT (2001) A summary of 20 CACNA1F mutations
704 identified in 36 families with incomplete X-linked congenital stationary night blindness,
705 and characterization of splice variants. Hum Genet 108:91-97.
706 Chichilnisky EJ (2001) A simple white noise analysis of neuronal light responses. Network-
707 Computation in Neural Systems 12:199-213.

Cui G, Meyer A, Calin-Jageman I, Neef J, Haeseleer F, Moser T, Lee A (2007) Ca2+-binding proteins tune Ca2+ -feedback to Cav1.3 Ca 2+ channels in auditory hair cells. Journal of Physiology 585:791-803.

Dieterich DC, Karpova A, Mikhaylova M, Zdobnova I, Konig I, Landwehr M, Kreutz M, Smalla KH, Richter K, Landgraf P, Reissner C, Boeckers TM, Zuschratter W, Spilker C, Seidenbecher CI, Garner CC, Gundelfinger ED, Kreutz MR (2008) Caldendrin-Jacob: a protein liaison that couples NMDA receptor signalling to the nucleus. PLoS Biol 6:e34.

Dunn FA, Wong RO (2012) Diverse strategies engaged in establishing stereotypic wiring patterns among neurons sharing a common input at the visual system's first synapse. J Neurosci 32:10306-10317.

Few AP, Nanou E, Scheuer T, Catterall WA (2011) Molecular Determinants of Ca(v)2.1 Channel Regulation by Calcium-binding Protein-1. Journal of Biological Chemistry 286:41917-41923.

Findeisen F, Minor DL (2010) Structural Basis for the Differential Effects of CaBP1 and Calmodulin on Ca(v)1.2 Calcium-Dependent Inactivation. Structure 18:1617-1631.

Ghosh KK, Bujan S, Haverkamp S, Feigenspan A, Wassle H (2004) Types of bipolar cells in the mouse retina (vol 469, pg 70, 2004). Journal of Comparative Neurology 476:202-203.

Gorny X, Mikhaylova M, Seeger C, Reddy PP, Reissner C, Schott BH, Helena Danielson U, Kreutz MR, Seidenbecher C (2012) AKAP79/150 interacts with the neuronal calcium-binding protein caldendrin. J Neurochem 122:714-726.

Habermann CJ, O'Brien BJ, Wassle H, Protti DA (2003) AII amacrine cells express L-type calcium channels at their output synapses. Journal of Neuroscience 23:6904-6913.

Haeseleer F, Palczewski K (2002) Calmodulin and Ca2+-binding proteins (CaBPs): Variations on a theme. In: Photoreceptors and Calcium, pp 303-317.

Haeseleer F, Imanishi Y, Maeda T, Possin DE, Maeda A, Lee A, Rieke F, Palczewski K (2004) Essential role of Ca2+-binding protein 4, a Ca(v)1.4 channel regulator, in photoreceptor synaptic function. Nature Neuroscience 7:1079-1087.

Haeseleer F, Sokal I, Verlinde C, Erdjument-Bromage H, Tempst P, Pronin A, Benovic J, Fariss R, Palczewski K (2000) Five members of a novel Ca2+-binding protein (CABP) Subfamily with Similarity to Calmodulin. Journal of Biological Chemistry 275:1247-1260.

Hardie J, Lee A (2016) Decalmodulation of Cav1 channels by CaBPs. Channels (Austin) 10:33-37.

Haverkamp S, Wassle H (2000) Immunocytochemical analysis of the mouse retina. Journal of Comparative Neurology 424:1-23.

Haverkamp S, Haeseleer F, Hendrickson A (2003a) A comparison of immunocytochemical markers to identify bipolar cell types in human and monkey retina. Visual Neuroscience 20:589-600.

Haverkamp S, Ghosh KK, Hirano AA, Wassle H (2003b) Immunocytochemical description of five bipolar cell types of the mouse retina. Journal of Comparative Neurology 455:463-476.

Haverkamp S, Specht D, Majumdar S, Zaidi NF, Brandstatter JH, Wasco W, Wassle H, Tom Dieck S (2008) Type 4 OFF cone bipolar cells of the mouse retina express calsenilin and contact cones as well as rods. J Comp Neurol 507:1087-1101.

Haynes LP, Tepikin AV, Burgoyne RD (2004) Calcium-binding protein 1 is an inhibitor of agonist-evoked, inositol 1,4,5-trisphosphate-mediated calcium signaling. Journal of Biological Chemistry 279:547-555.

Kaneko A, Pinto LH, Tachibana M (1989) Transient calcium current of retinal bipolar cells of the mouse. J Physiol 410:613-629.

Khan AO (2013) CABP4 Mutations Do Not Cause Congenital Stationary Night Blindness. Ophthalmology.

758 Khan AO, Alrashed M, Alkuraya FS (2012) Clinical characterisation of the CABP4-related retinal
759 phenotype. British Journal of Ophthalmology Oct. 31. Epub ahead of print.
760 Kim KJ, Rieke F (2001) Temporal contrast adaptation in the input and output signals of
761 salamander retinal ganglion cells. J Neurosci 21:287-299.
762 Kim KY, Scholl ES, Liu X, Shepherd A, Haeseleer F, Lee A (2014) Localization and expression
763 of CaBP1/caldendrin in the mouse brain. Neuroscience 268:33-47.
764 Lee A, Westenbroek RE, Haeseleer F, Palczewski K, Scheuer T, Catterall WA (2002)
765 Differential modulation of Ca(v)2.1 channels by calmodulin and Ca2+-binding protein 1.
766 Nature Neuroscience 5:210-217.
767 Li C, Enomoto M, Rossi AM, Seo MD, Rahman T, Stathopulos PB, Taylor CW, Ikura M, Ames
768 JB (2013) CaBP1, a neuronal Ca2+ sensor protein, inhibits inositol trisphosphate
769 receptors by clamping intersubunit interactions. Proc Natl Acad Sci U S A 110:8507-
770 8512.
771 Lin B, Masland RH (2005) S(y)naptic contacts between an identified type of ON cone bipolar
772 cell and ganglion cells in the mouse retina. European Journal of Neuroscience 21:1257-
773 1270.
774 Mansergh F, Orton NC, Lalonde MR, Stell WK, Tremblay F, Barnes S, Rancourt DE, Bech-
775 Hansen NT (2005) Mutation of the calcium channel gene Cacna1f disrupts calcium
776 signaling, synaptic transmission and cellular organization in mouse retina. Human
777 Molecular Genetics 14:3035-3046.
778 Menger N, Seidenbecher CI, Gundelfinger ED, Kreutz MR (1999) The cytoskeleton-associated
779 neuronal calcium-binding protein caldendrin is expressed in a subset of amacrine,
780 bipolar and ganglion cells of the rat retina. Cell and Tissue Research 298:21-32.
781 Morgan JL, Soto F, Wong RO, Kerschensteiner D (2011) Development of cell type-specific
782 connectivity patterns of converging excitatory axons in the retina. Neuron 71:1014-1021.
783 Murphy GJ, Rieke F (2006) Network variability limits stimulus-evoked spike timing precision in
784 retinal ganglion cells. Neuron 52:511-524.
785 Pan ZH (2000) Differential expression of high- and two types of low-voltage- activated calcium
786 currents in rod and cone bipolar cells of the rat retina. Journal of Neurophysiology
787 83:513-527.
788 Pan ZH, Hu HJ, Perring P, Andrade R (2001) T-type Ca2+ channels mediate neurotransmitter
789 release in retinal bipolar cells. Neuron 32:89-98.
790 Pang JJ, Gao F, Wu SM (2003) Light-evoked excitatory and inhibitory synaptic inputs to ON and
791 OFF alpha ganglion cells in the mouse retina. J Neurosci 23:6063-6073.
792 Pignatelli V, Strettoi E (2004) Bipolar cells of the mouse retina: a gene gun, morphological
793 study. J Comp Neurol 476:254-266.
794 Rieke F (2001) Temporal contrast adaptation in salamander bipolar cells. J Neurosci 21:9445-
795 9454.
796 Rieke F, Lee A, Haeseleer F (2008) Characterization of Ca2+-Binding Protein 5 Knockout
797 Mouse Retina. Investigative Ophthalmology & Visual Science 49:5126-5135.
798 Schrauwen I, Helfmann S, Inagaki A, Predoehl F, Tabatabaiefar MA, Picher MM, Sommen M,
799 Seco CZ, Oostrik J, Kremer H, Dheedene A, Claes C, Fransen E, Chaleshtori MH,
800 Coucke P, Lee A, Moser T, Van Camp G (2012) A mutation in CABP2, expressed in
801 cochlear hair cells, causes autosomal-recessive hearing impairment. Am J Hum Genet
802 91:636-645.
803 Schwartz GW, Okawa H, Dunn FA, Morgan JL, Kerschensteiner D, Wong RO, Rieke F (2012)
804 The spatial structure of a nonlinear receptive field. Nat Neurosci 15:1572-1580.
805 Seidenbecher CI, Langnaese K, Sanmarti-Vila L, Boeckers TM, Smalla KH, Sabel BA, Garner
806 CC, Gundelfinger ED, Kreutz MR (1998) Caldendrin, a novel neuronal calcium-binding
807 protein confined to the somato-dendritic compartment. Journal of Biological Chemistry
808 273:21324-21331.

Seidenbecher CI, Landwehr M, Smalla KH, Kreutz M, Dieterich DC, Zuschratter W, Reissner C, Hammarback JA, Bockers TM, Gundelfinger ED, Kreutz MR (2004) Caldendrin but not calmodulin binds to light chain 3 of MAP1A/B: an association with the microtubule cytoskeleton highlighting exclusive binding partners for neuronal Ca(2+)-sensor proteins. J Mol Biol 336:957-970.

Shaltiel L, Paparizos C, Fenske S, Hassan S, Gruner C, Rotzer K, Biel M, C.A. W-S (2012) Complex Regulation of Voltage-dependent Activation and Inactivation Properties of Retinal Voltage-gated Cav1.4 L-type Ca2+ Channels by Ca2+-binding Protein 4 (CaBP4).

. Journal of Biological Chemistry 287:36312-36321.

Singer JH, Diamond JS (2003) Sustained Ca2+ entry elicits transient postsynaptic currents at a retinal ribbon synapse. Journal of Neuroscience 23:10923-10933.

Sokal I, Haeseleer F (2011) Insight into the Role of Ca(2+)-Binding Protein 5 in Vesicle Exocytosis. Investigative Ophthalmology & Visual Science 52:9131-9141.

Sokal I, Li N, Verlinde C, Haeseleer F, Baehr W, Palczewski K (2000) Ca2+-binding proteins in the retina: from discovery to etiology of human disease. Biochimica Et Biophysica Acta-Molecular Cell Research 1498:233-251.

Strom TM, Nyakatura G, Apfelstedt-Sylla E, Hellebrand H, Lorenz B, Weber BHF, Wutz K, Gutwillinger N, Ruther K, Drescher B, Sauer C, Zrenner E, Meitinger T, Rosenthal A, Meindl A (1998) An L-type calcium-channel gene mutated in incomplete X-linked congenital stationary night blindness. Nature Genetics 19:260-263.

van Wyk M, Wassle H, Taylor WR (2009) Receptive field properties of ON- and OFF-ganglion cells in the mouse retina. Vis Neurosci 26:297-308.

Wassle H (2004) Parallel processing in the mammalian retina. Nat Rev Neurosci 5:747-757.

Wassle H, Puller C, Muller F, Haverkamp S (2009) Cone contacts, mosaics, and territories of bipolar cells in the mouse retina. J Neurosci 29:106-117.

Welsby PJ, Wang H, Wolfe JT, Colbran RJ, Johnson ML, Barrett PQ (2003) A mechanism for the direct regulation of T-type calcium channels by Ca2+/calmodulin-dependent kinase II. J Neurosci 23:10116-10121.

Wutz K, Sauer C, Zrenner E, Lorenz B, Alitalo T, Broghammer M, Hergersberg M, de La Chapelle A, Weber BHF, Wissinger B, Meindl A, Pusch CM (2002) Thirty distinct CACNA1F mutations in 33 families with incomplete type of XLCSNB and Cacna1f expression profiling in mouse retina. European Journal of Human Genetics 10:449-456.

Yang J, McBride S, Mak DOD, Vardi N, Palczewski K, Haeseleer F, Foskett JK (2002) Identification of a family of calcium sensors as protein ligands of inositol trisphosphate receptor Ca2+ release channels. Proceedings of the National Academy of Sciences of the United States of America 99:7711-7716.

Yang PS, Alseikhan BA, Hiel H, Grant L, Mori MX, Yang WJ, Fuchs PA, Yue DT (2006) Switching of Ca2+-dependent inactivation of Ca(V)1.3 channels by calcium binding proteins of auditory hair cells. Journal of Neuroscience 26:10677-10689.

Zeitz C, Kloeckener-Gruissem B, Forster U, Kohl S, Magyar I, Wissinger B, Matyas G, Borruat FX, Schorderet DF, Zrenner E, Munier FL, Berger W (2006) Mutations in CABP4, the gene encoding the Ca2+-binding protein 4, cause autosomal recessive night blindness. American Journal of Human Genetics 79:657-667.

Zhou H, Kim SA, Kirk EA, Tippens AL, Sun H, Haeseleer F, Lee A (2004) Ca2+-binding protein-1 facilitates and forms a postsynaptic complex with Ca(v)1.2 (L-Type) Ca2+ channels. Journal of Neuroscience 24:4698-4708.

Table 1. Identified CaBP1/CD or CaBP2 expressing cell types in the mouse retina.

Cell type / Marker	CaBP1	CaBP2
OFF type 1 BP / NK3R	+	+
OFF type 2 BP / NK3R and Syt2	+	
OFF type 3 BP (3a and 3b) / CaBP5		
OFF type 4 BP / Calsenilin		
ON type 5 BP / CaBP5		
ON type 6 BP / Syt 2		+
ON type 7 BP / Gustducin-GFP		
Rod BP / CaBP5		
Amacrine cells / Calretinin	+	

Retinal cell types tested for the expression of CaBP1 and CaBP2 and labeled with the indicated markers.

Table 2. Quantification of the number of Ctbp2-labeled ribbons.

	Number / 25 μm^2					
	Ribbons in OPL	*p* value	Ribbons in NK3R-labeled outer IPL	*p* value	Ribbons in Syt2-labeled inner IPL	*p* value
WT	8.58 ± 0.30	1	16.33 ± 0.45	1	13.33 ± 0.42	1
Cabp1$^{-/-}$	8.12 ± 0.27	0.26	16.04 ± 0.49	0.66	14.16 ± 0.53	0.22
Cabp2$^{-/-}$	8.25 ± 0.21	0.36	16.75 ± 0.47	0.53	14.54 ± 0.53	0.08

Retinal wholemount, as shown in figures 4 and 6, from 4 mice for each phenotype were analyzed by confocal microscopy. Ctbp2-labeled ribbons were counted in images of six areas of 25 μm^2 for each mouse in the OPL. Ctbp2-labeled puncta were also quantified in the NK3R-labeled sublamina containing type 1 and type2 OFF bipolar cells axon terminals or in Syt2-labeled sublaminae of the inner IPL containing the type 6 ON bipolar cells. Numbers represent mean ± s.e. (n=24). Statistical comparisons with WT mice were performed using the Student's t-test.

Figure 1

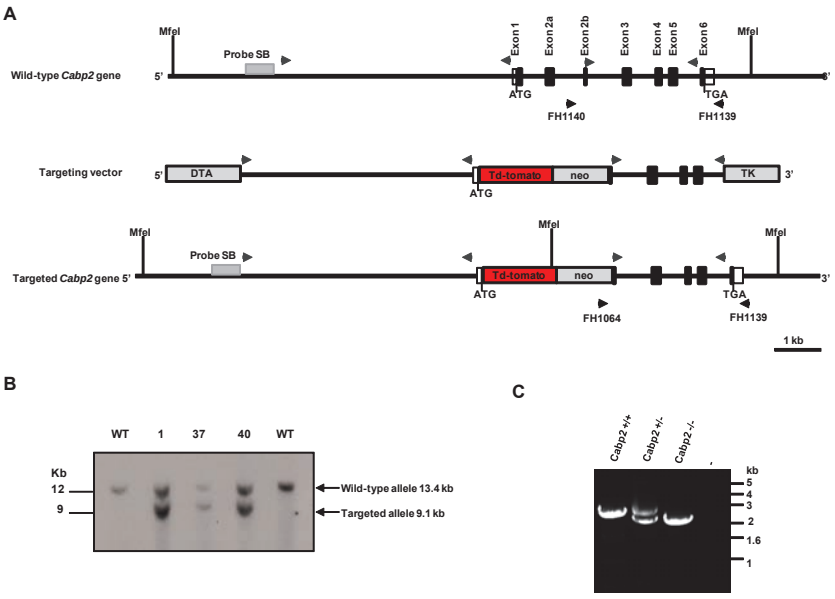

Figure 2

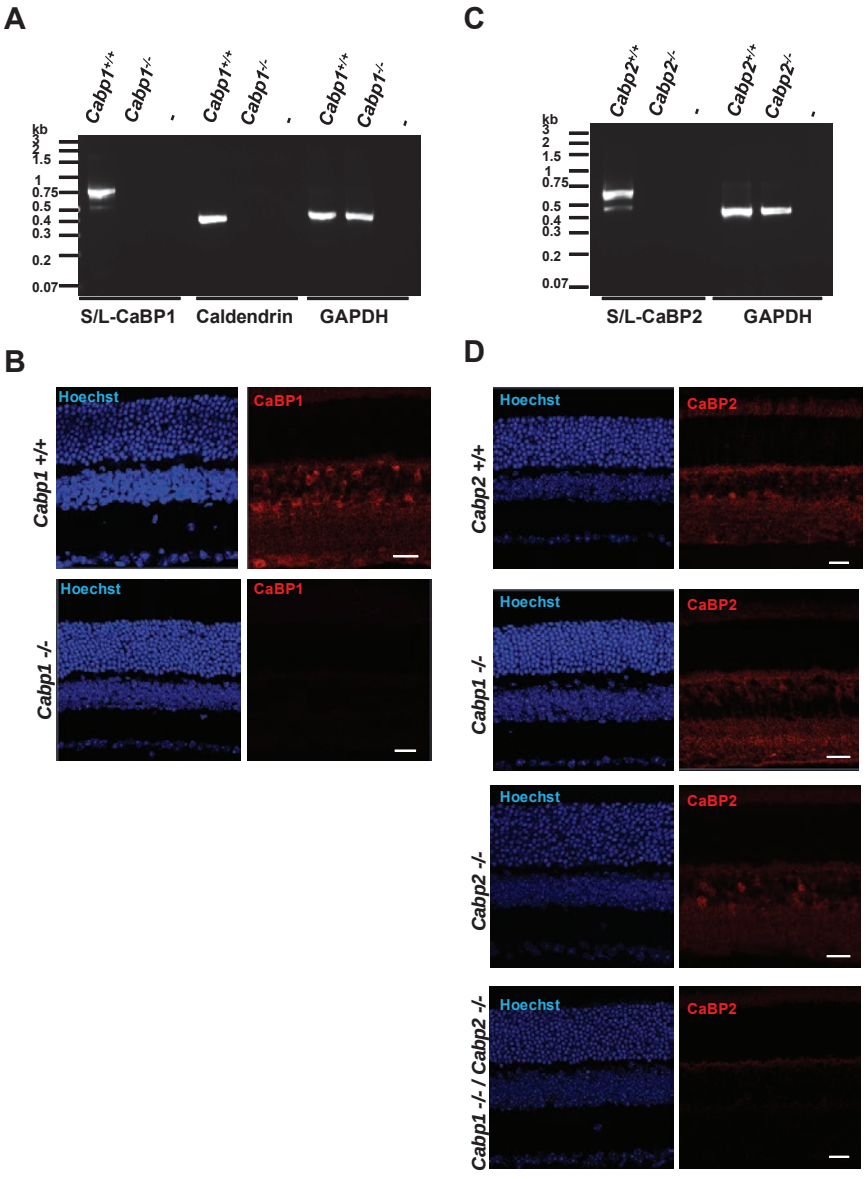

Figure 3

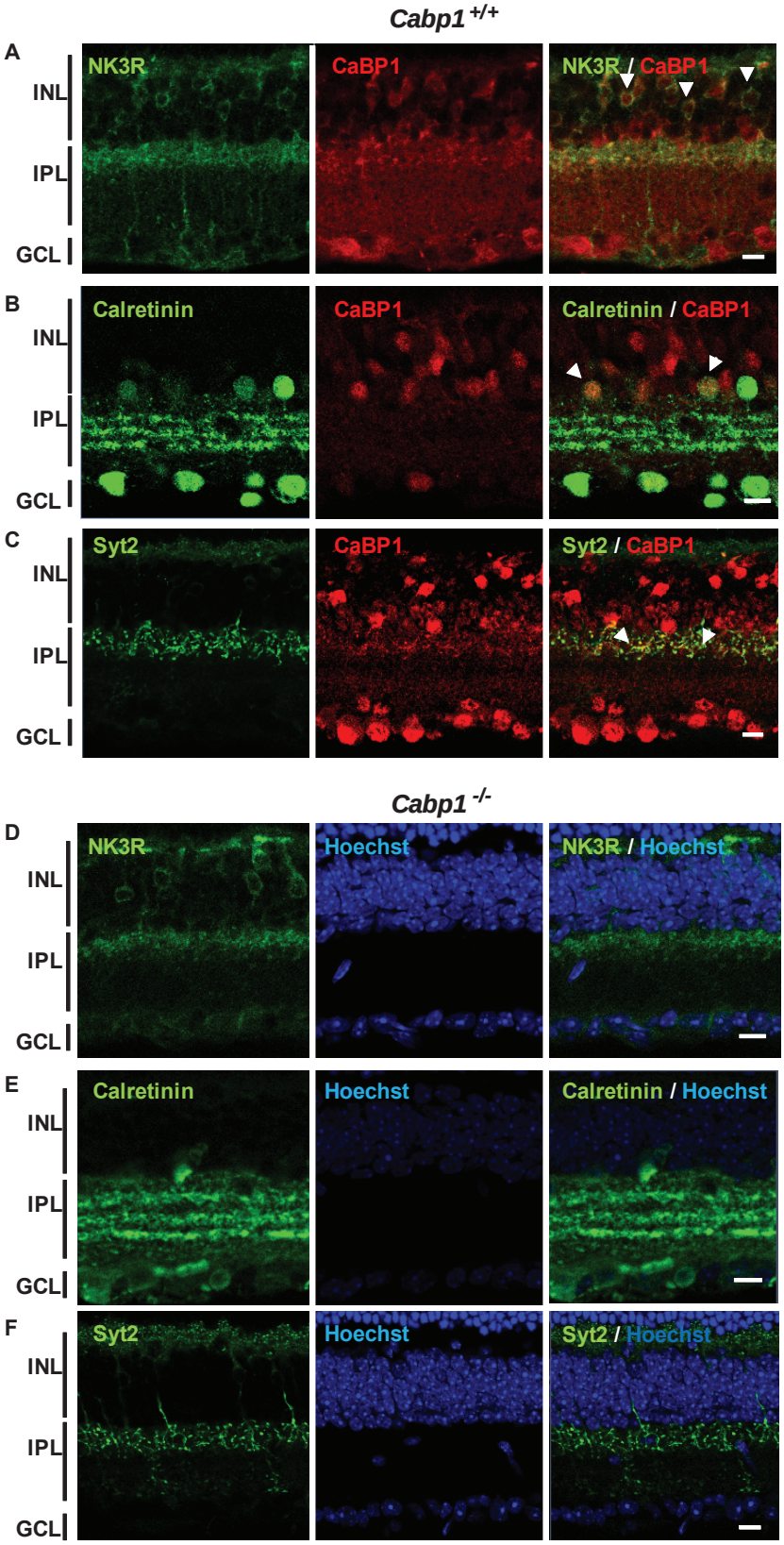

Figure 4

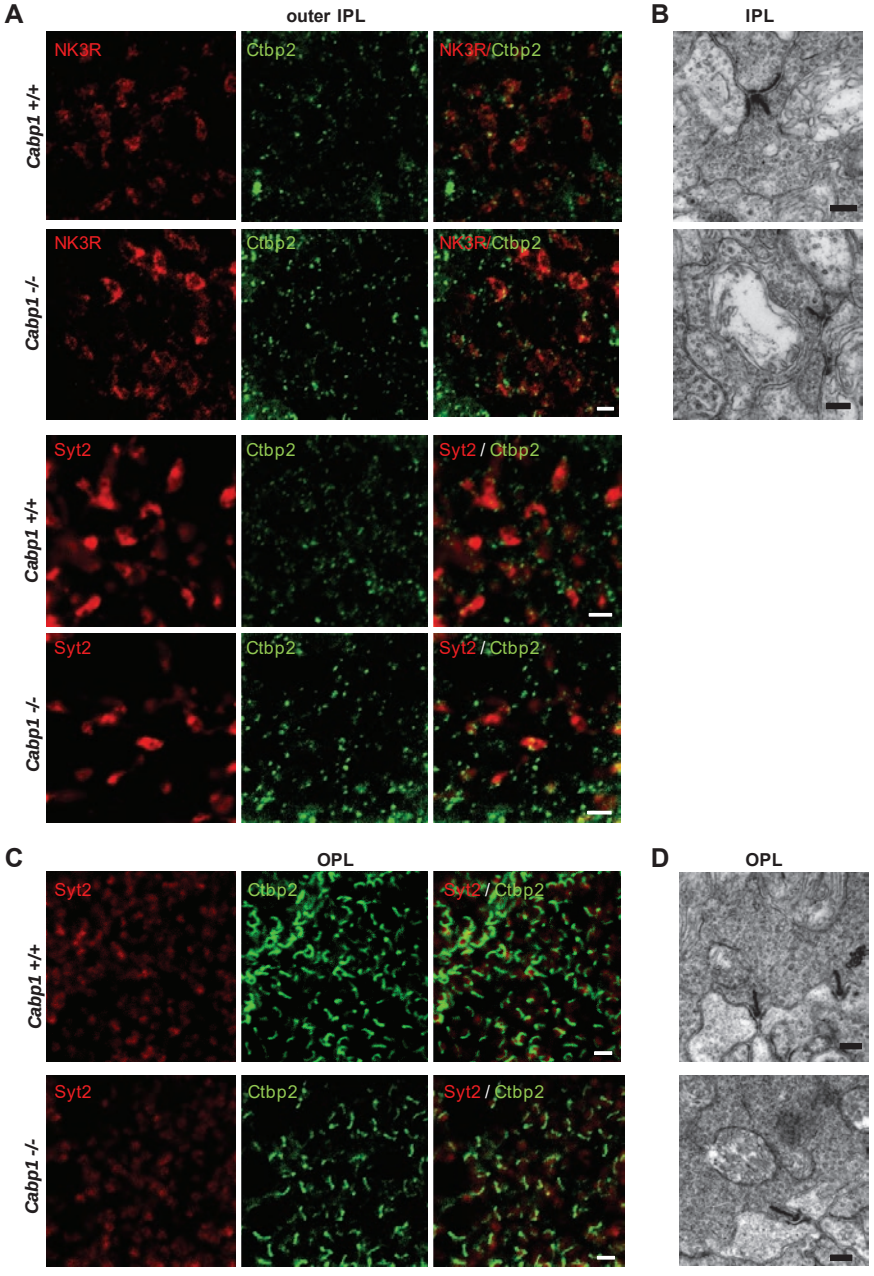

Figure 5

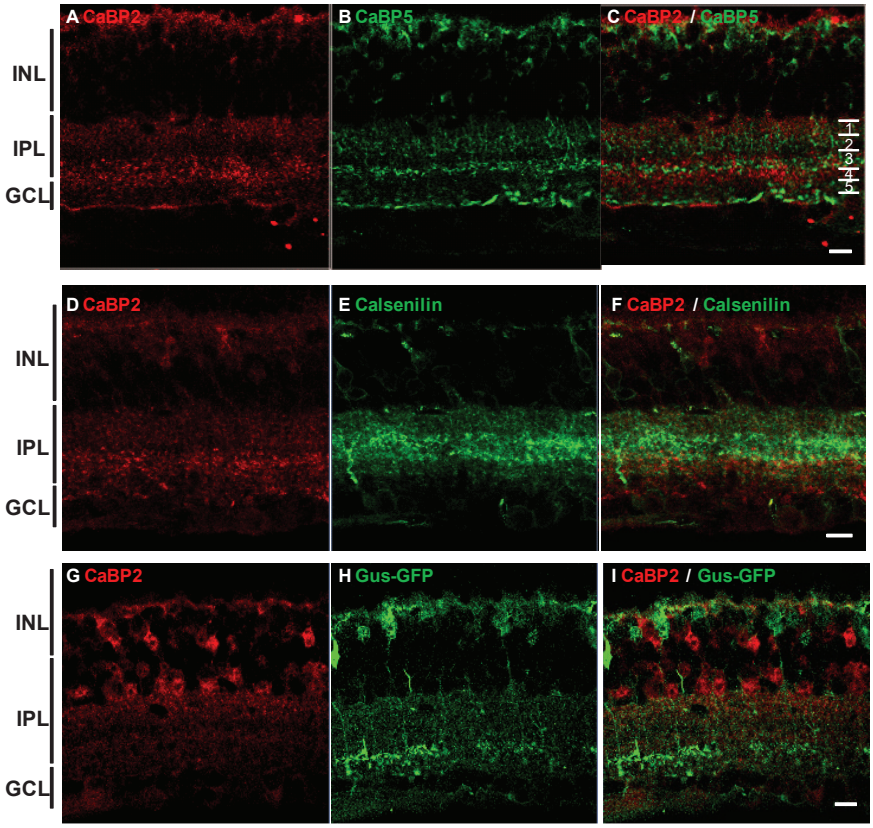

Figure 6

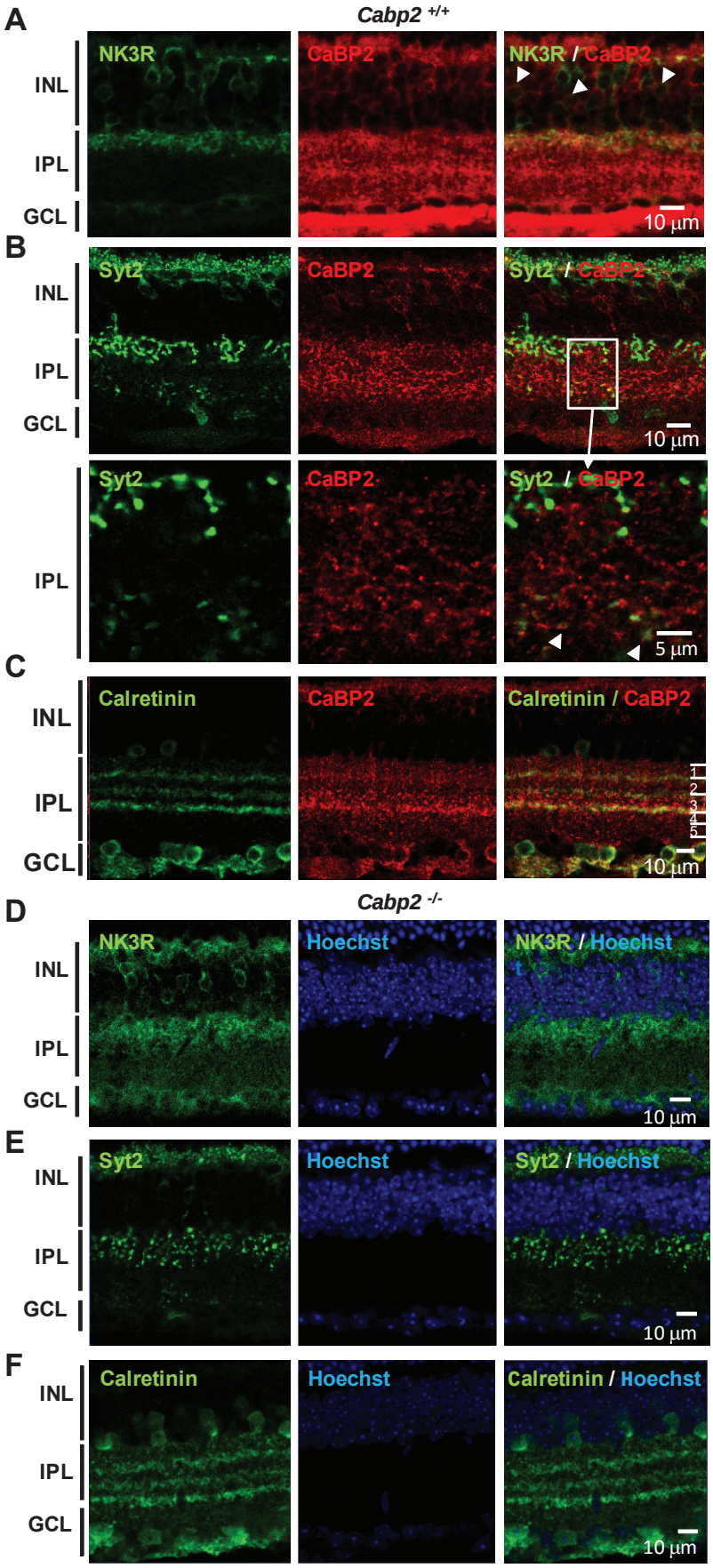

Figure 7

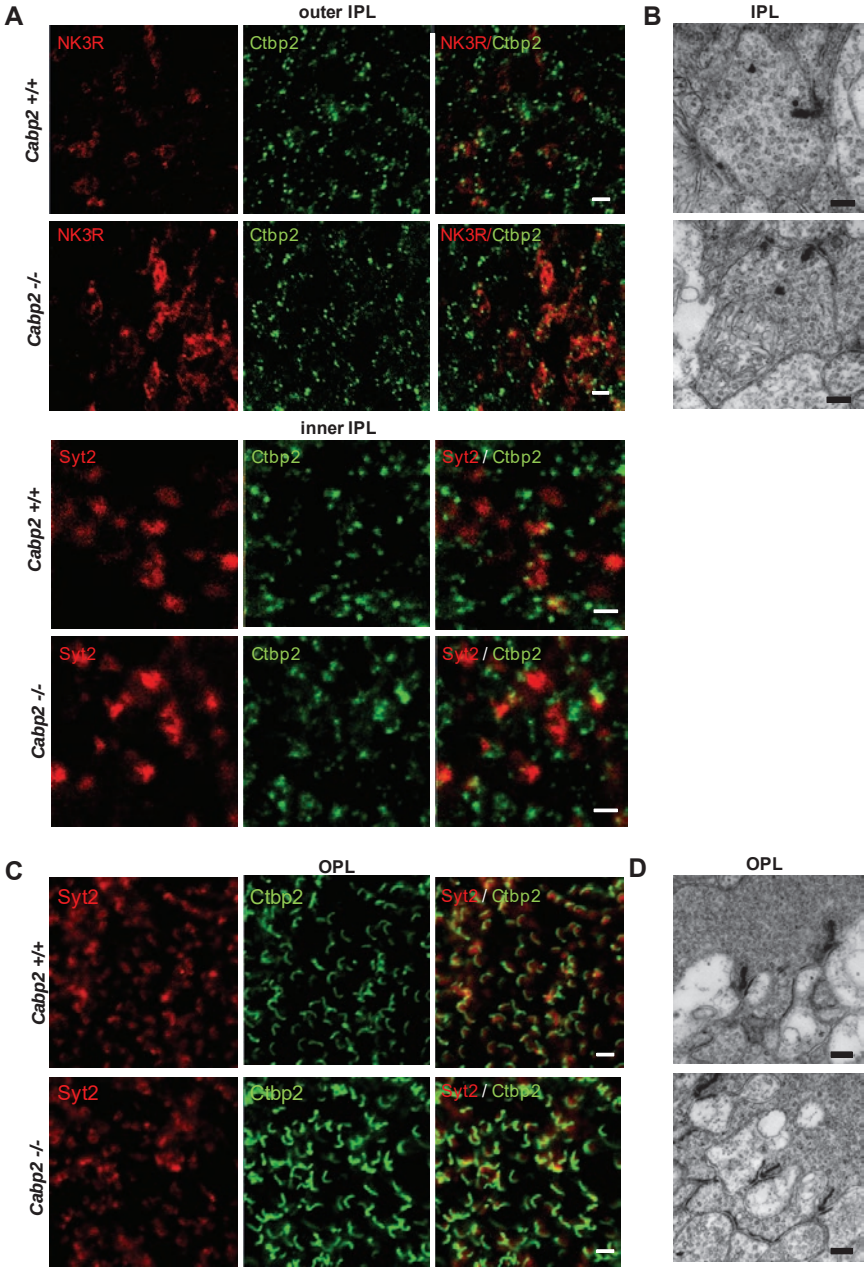

Figure 8

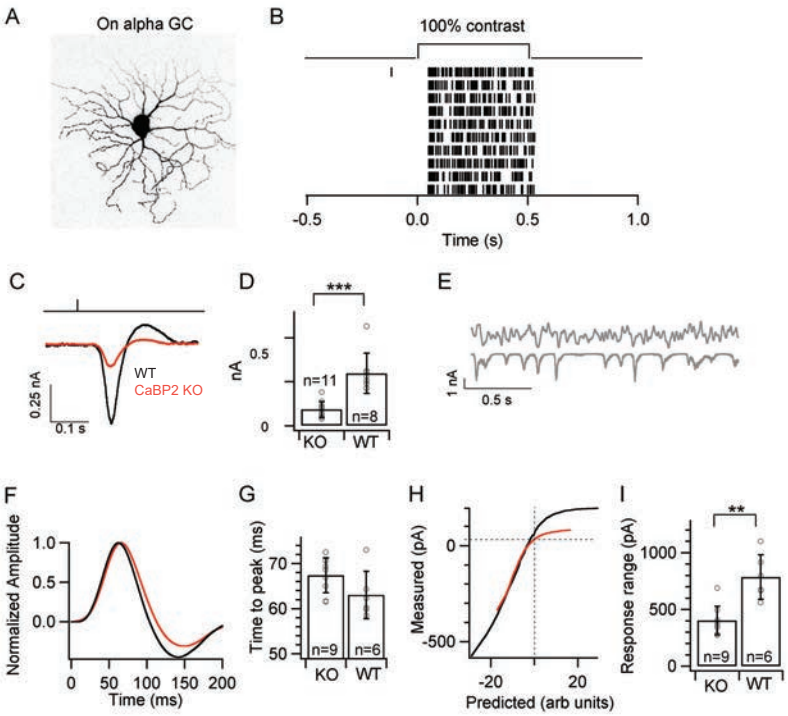

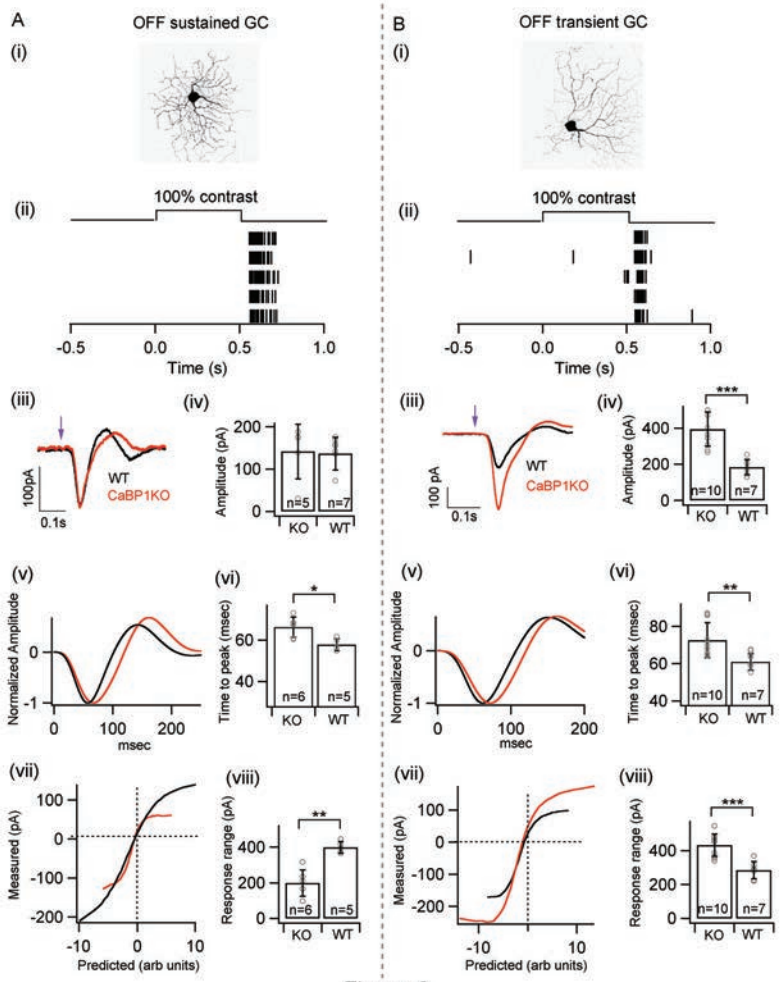

Figure. 9

Figure 10

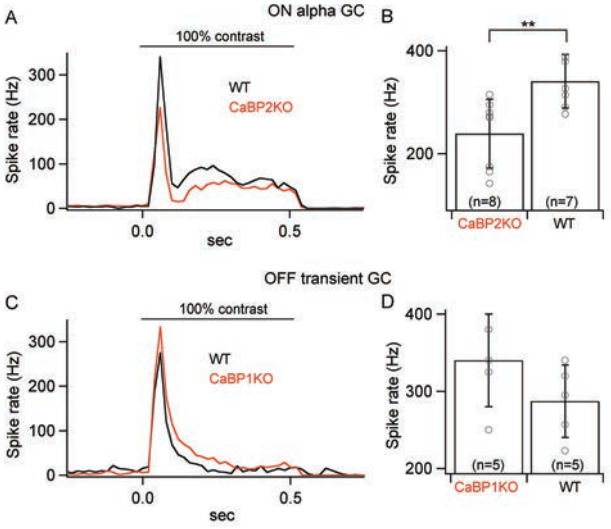

Figure 11